

A superstable time-discrete scheme for the numerical integration of viscous constitutive equations

P. Royis *

August 31, 2022

Abstract

The general framework of the paper deals with the finite element modelling of mechanical problems involving viscous materials such as bitumen or bituminous concrete. Its aim is to present a second-order-accurate discrete scheme which remains unconditionally superstable when used for the time discretization of the linear and non-linear viscoelastic constitutive equations considered. After stating the space- and time-continuous mechanical problem we focus on the time discretization of these equations, considering three different schemes. For both of them sufficiently small values of the time step are required in order to ensure the superstability, whereas the third remains unconditionally superstable. Eventually, some numerical results are presented.

KEY WORDS: finite element method; viscous constitutive equations; time-discrete scheme; stability; superstability

1 Introduction

The general framework of this paper deals with the finite element modelling of mechanical problems involving viscous materials, such as bitumen or bituminous concrete. These materials are often used in civil engineering (asphalt pavements, kernels of dams, . . .) and taking the rate-dependent component of their behaviour into account is necessary if one wants to lay out the corresponding structures correctly. Provided one restricts the frame of the study to small perturbations (i.e. small strains and small displacements), this viscous component can then be approached¹ by linear or non-linear viscoelastic constitutive equations such as those considered in this paper.

*Ecole Nationale des Travaux Publics de l'Etat, Département Génie Civil et Bâtiment (URA CNRS 1652), rue M. Audin, 69518 Vaulx-en-Velin Cedex, France.

The main difficulty when using such equations for finite element computations lies in their integration over finite time steps. For that purpose robust time-discrete schemes are needed if one wants to obtain accurate numerical approximations at a reasonable cost. The term ‘robust’ means here that those schemes remain stable for sufficiently large values of the time step. More generally speaking, the bringing into play of robust schemes is advisable as soon as unelastic constitutive laws are considered. That subject has been studied intensively as regards both rate-dependent and rate-independent equations.^{2–5} For instance, it is well known that explicit integration formulae showing good stability properties when used for rate-independent constitutive laws^{2,3} can turn out to be excessively expensive for rate-dependent ones whenever their stability regions become too small. A first way of avoiding this drawback consists in using semi- or fully implicit schemes which bring unconditional stability.⁴ This leads to solve iteratively a non-linear system of equations as soon as non-linear constitutive relations are considered. Another approach using semi-implicit Runge-Kutta methods has been suggested by Rosenbrock⁶ in order to increase stability while avoiding fully implicit schemes. Halfway between explicit and implicit methods are also the forward gradient schemes, which have been successfully implemented in finite element codes when combined with efficient time-stepping strategies.⁵ But both Rosenbrock and forward gradient procedures are not, in general, unconditionally stable. Although some of the viscous constitutive relations considered in the paper are non-linear, its topic comes within the framework of the first approach. However, it is well known that when the size Δt of the step increases some oscillations of the numerical solutions can appear even if an unconditionally stable scheme is used, such a phenomenon resulting then from a loss of superstability.⁷ The main objective of the paper is to present a $\mathcal{O}(\Delta t^2)$ -accurate discrete scheme which does not have this drawback, that is to say, which remains unconditionally superstable (and consequently unconditionally stable) when used for the time discretization of the viscoelastic constitutive equations considered.

This paper consists of four main sections. The first one is devoted to the statement of the time-continuous mechanical problem. In addition to the above-mentioned small perturbations, the transformations of the materially simple continuum Ω are assumed to be quasistatic, and only the mechanical aspects of the resulting problems are taken into account, which means that the influence of thermal coupling effects on the behaviour of Ω is not studied in this paper. Three viscous constitutive models are considered. The first one consists in a non-ageing anisotropic linear viscoelastic body.⁸ The other two,^{9,10} which are isotropic and non-linear, are

rewritten in a unified form for concision's sake.

The second section deals with general considerations relating to the weak formulation of the time-discretized mechanical problem, whereas the third one focuses on the particularly important point constituted by the time discretization of the constitutive equations. We first define both concepts of stability and superstability by considering a linear ordinary differential equation, and illustrate them by examining three classical Runge-Kutta schemes. Three different schemes used for the time discretization of the constitutive equations and denoted as S1, S2 and S3, respectively, are then described. The first one,^{8,11} based upon the assumption of linear variations of the stresses over the time step, has $\mathcal{O}(\Delta t^2)$ accuracy for the models considered. It remains unconditionally stable, but sufficiently small values of Δt are required in order to have the superstability. The second one is the classical θ -scheme, the well-known properties of which are recalled. Finally the original scheme S3 has $\mathcal{O}(\Delta t^2)$ accuracy and is unconditionally superstable (and consequently unconditionally stable) when used for the time discretization of the models considered.

Some numerical results are presented in the last section. A set of computations carried out by using a single four-nodes quadrilateral element for the numerical simulation of homogeneous axisymmetric triaxial compression tests is first analysed, before dealing with the problem of the expanding viscoelastic hollow cylinder together with that of the bending viscoelastic beam.

2 The time-continuous mechanical problem

2.1 General considerations

Let Ω be a materially simple continuum, the motion of which is studied over the time interval $[0, T]$. As mentioned in the introduction above, the influence of thermal coupling effects on the behaviour of Ω is not within the scope of this paper, in which only the mechanical aspects of the problems considered will be tackled. We shall denote as Γ the boundary of Ω , and as \mathbf{n} the outer unit normal to Γ . Ω is assumed to be an open, bounded and simply connected region of \mathbb{R}^3 , and its boundary Γ is assumed to be lipschitz-continuous. The successive configurations of this continuum will be observed with respect to the same fixed orthonormal frame, and we shall assume small strains and small displacements. Eventually, we consider only quasistatic problems, for which the acceleration may be ignored. The mechanical problem stated in the following subsection consists then in determining the history $\mathbf{u}(t, \cdot)$ of the displacement field of

the continuum Ω over the time interval $[0, T]$.

2.2 The space- and time-continuous mechanical problem

Let $\mathbf{b}(t, \cdot)$ be the vectorial field at time t of the body forces acting per volume unit in Ω . We shall denote as $\Gamma_1(t)$ the part of Γ on which we have, at time t , the essential boundary conditions $\mathbf{u}|_{\Gamma_1(t)} = \mathbf{u}_i$, where $\mathbf{u}_i(t, \cdot)$ is the field of the displacements given on $\Gamma_1(t)$, and as $\Gamma_2(t)$ the part of Γ on which the values of the stress vector are prescribed at the same time. We assume that $\Gamma_1(t)$ and $\Gamma_2(t)$ constitute, at every time t , a partition of Γ such that $\Gamma_1(t)$ has at least three points, and we denote as $\mathbf{g}(t, \cdot)$ the values of the stress vector given on $\Gamma_2(t)$.

Let now $\varepsilon(t, \cdot)$ be the mechanical component of the linearized tensorial field of the small strains in Ω at time t , and let $\sigma(t, \cdot)$ be the tensorial field of the Cauchy stresses in Ω at the same time. This paper focuses on the finite element modelling of geomaterials, such as bitumen or bituminous concrete, the behaviour of which is described by a linear or non-linear viscoelastic constitutive law. The constitutive equations considered in this paper, the expressions of which are detailed in the following subsection, can be written in the concise form

$$\dot{\varepsilon} = \mathbf{F}(\dot{\sigma}, \sigma, \mathcal{H}) \quad (1)$$

where $\dot{\varepsilon}$ and $\dot{\sigma}$ are the rates of ε and σ , respectively, and where \mathcal{H} denotes the set of memory parameters different from σ .

Then the problem which consists in determining the history $\mathbf{u}(t, \cdot)$ of the displacements of Ω over the time interval $[0, T]$ is governed by the following set of equations

$$\left\{ \begin{array}{l} (2.1a) \quad \mathbf{div}_x \sigma(t, x) = -\mathbf{b}(t, x) \\ (2.1b) \quad \sigma^T(t, x) = \sigma(t, x) \\ (2.2) \quad \dot{\varepsilon}(t, x) = \mathbf{F}(\dot{\sigma}(t, x), \sigma(t, x), \mathcal{H}(t, x)) \\ (2.3a) \quad \mathbf{u}(t, x) = \mathbf{u}_i(t, x) \quad \text{on } \Gamma_1(t) \times]0, T[\\ (2.3b) \quad \sigma(t, x) \cdot \mathbf{n} = \mathbf{g}(t, x) \quad \text{on } \Gamma_2(t) \times]0, T[\\ (2.4a) \quad \mathbf{u}(0, x) = \mathbf{u}_0(x) \\ (2.4b) \quad \sigma(0, x) = \sigma_0(x) \end{array} \right\} \begin{array}{l} \text{in } \Omega \times]0, T[\\ \\ \\ \text{in } \Omega \end{array} \quad (2)$$

Equations (2.1a) and (2.1b) arise from the application of the principle of balance of linear and angular momentum, in the absence of body and surface couples. Equation (2.2) is the formulation of the constitutive law of the viscous materially simple continuum Ω , under the assumption of small transformations. The boundary conditions are given by equations (2.3a) and (2.3b). Finally, the relations (2.4a) and (2.4b) provide initial conditions of the problem.

In the following subsection we give the detailed expression of the viscous constitutive equations (1).

2.3 The constitutive equations

To begin with we consider a non-ageing anisotropic linear viscoelastic model. Based upon the assumption of a finite spectral decomposition of the retardation tensor, it generalizes⁸ the expression of this decomposition coming from thermodynamical considerations¹ by freeing from the Onsager principle. Its general formulation is given in the following paragraph.

Let $(i, j, k, l) \in \{1, 2, 3\}^4$ be any given set of indices and let ε_{ijkl} denote the contribution to the component ε_{ij} of ε , due to the history of the component σ_{kl} of σ .

Then the correspondence between the histories of σ_{kl} and ε_{ijkl} can be represented⁸ by the one-dimensional analogical model shown on the figure 1, where the parameters $k_{ijkl}^{(\cdot)}$ and $\eta_{ijkl}^{(\cdot)}$ represent the stiffnesses of the springs and the viscosities of the dash-pots, respectively.

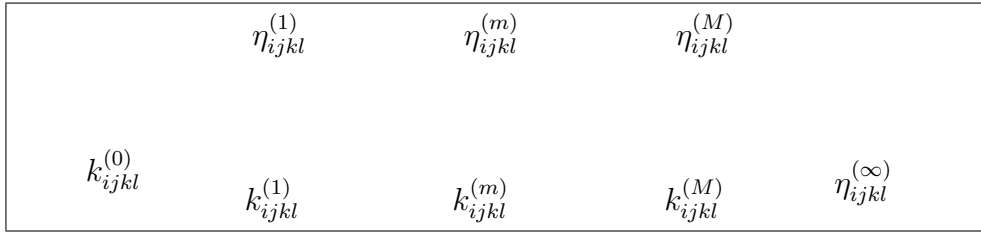


Figure 1. Analogical model relating to the correspondence between σ_{kl} and ε_{ijkl}

Its constitutive equation relating to time t is given, without any summation on k and l , by

$$\dot{\varepsilon}_{ijkl}(t) = \frac{\dot{\sigma}_{kl}(t)}{k_{ijkl}^{(0)}} + \sum_{m=1}^{m=M} \dot{\varepsilon}_{ijkl}^{(m)}(t) + \frac{\sigma_{kl}(t)}{\eta_{ijkl}^{(\infty)}} \quad (3)$$

with, if $M \in \mathbb{N}^*$, $\forall m \in \{1, \dots, M\}$ and without any summation on i, j, k and l

$$\sigma_{kl}(t) = k_{ijkl}^{(m)} \varepsilon_{ijkl}^{(m)}(t) + \eta_{ijkl}^{(m)} \dot{\varepsilon}_{ijkl}^{(m)}(t) \quad (4)$$

and we shall agree to drop the summation on m in equation (3) if $M = 0$.

In all the following, $\forall (i, j, k, l) \in \{1, 2, 3\}^4$, $\forall m \in \{1, \dots, M\}$ and without any summation on i, j, k and l , we shall put

$$J_{ijkl}^{(0)} = \frac{1}{k_{ijkl}^{(0)}} \quad J_{ijkl}^{(\infty)} = \frac{1}{\eta_{ijkl}^{(\infty)}} \quad J_{ijkl}^{(m)} = \frac{1}{k_{ijkl}^{(m)}} \quad \lambda_{ijkl}^{(m)} = \frac{k_{ijkl}^{(m)}}{\eta_{ijkl}^{(m)}} \quad (5)$$

The general equations of the non-ageing anisotropic linear viscoelastic model are then obtained from (3) and (4), after summation on indices k and l of the various contributions ε_{ijkl} to the component ε_{ij} of ε . We obtain, $\forall (i, j) \in \{1, 2, 3\}^2$,

$$\dot{\varepsilon}_{ij}(t) = J_{ijkl}^{(0)} \dot{\sigma}_{kl}(t) + \sum_{m=1}^{m=M} \dot{\varepsilon}_{ij}^{(m)}(t) + J_{ijkl}^{(\infty)} \sigma_{kl}(t) \quad (6)$$

where the strains $\varepsilon_{ij}^{(m)}(t)$, $(i, j) \in \{1, 2, 3\}^2$, $m \in \{1, \dots, M\}$, are solutions (if $M \in \mathbb{N}^*$) of the following equations

$$\left\{ \begin{array}{l} \varepsilon_{ij}^{(m)}(t) = \sum_{k=1}^{k=3} \sum_{l=1}^{l=3} \varepsilon_{ijkl}^{(m)}(t) \\ \text{with } \left\{ \begin{array}{l} \forall (k, l) \in \{1, 2, 3\}^2 \text{ and without any summation on } k \text{ and } l : \\ \frac{\dot{\varepsilon}_{ijkl}^{(m)}(t)}{\lambda_{ijkl}^{(m)}} + \varepsilon_{ijkl}^{(m)}(t) = J_{ijkl}^{(m)} \sigma_{kl}(t) \end{array} \right. \end{array} \right. \quad (7)$$

Let us now focus on the non-linear viscoelastic model of Maxwell-Norton-Hoff (e.g. see Friaâ⁹) together with a generalization of this model proposed by Di Benedetto¹⁰ for describing the behaviour of bitumen. Both of these models, which are isotropic, have been developed by their authors for incompressible media, and therefore they cannot be used in their original form for one-field (displacement or velocity) finite element computations. To avoid to resort to a two-fields finite element formulation, we suggest to modify the elastic component of these models in order to make it slightly compressible, whereas the unchanged viscous one keeps its incompressible feature.

The constitutive equations relating to the thus modified Maxwell-Norton-Hoff model are then as follows

$$\dot{\varepsilon}(t) = \frac{1 - 2\nu}{E} \dot{\sigma}_m(t) \mathbf{I}_2 + \frac{1 + \nu}{E} \dot{\mathbf{s}}(t) + \left(\frac{1}{\eta_0} + \frac{\|\mathbf{s}(t)\|^\alpha}{\eta} \right) \mathbf{s}(t) \quad (8)$$

where $E > 0$, $\nu \in] - 1, 1/2[$, $\eta_0 > 0$, $\eta > 0$ and $\alpha > 0$ are the five parameters of the model, and where \mathbf{I}_2 denotes the second-order unit tensor, \mathbf{s} denotes the deviatoric part of the Cauchy stress tensor σ , defined by $\mathbf{s} = \sigma - \sigma_m \mathbf{I}_2$ with $3\sigma_m = \text{tr}\sigma$, and $\|\mathbf{s}\|$ is the Euclidian norm of \mathbf{s} defined by $\|\mathbf{s}\| = \sqrt{s_{ij}s_{ij}}$. A nearly incompressible behaviour will be obtained when $\nu = 1/2 - \nu_\epsilon$, for sufficiently small values of the strictly positive constant ν_ϵ .

As to the modified model of Di Benedetto, it is given by the following expression

$$\dot{\varepsilon}(t) = \frac{1 - 2\nu}{E(t)} \dot{\sigma}_m(t) \mathbf{I}_2 + \frac{1 + \nu}{E(t)} \dot{\mathbf{s}}(t) + \frac{1}{\eta(t)} \mathbf{s}(t) \quad (9)$$

with

$$\begin{cases} E(t) = E_1 \left[1 + \left(2 \frac{\|\mathbf{s}(t)\|}{E_0} \right)^2 \right]^{\frac{1}{2}} & E_1 = \frac{3}{2} E_0 \\ \eta(t) = \eta_1 \left[1 + \left(\frac{\|\mathbf{s}(t)\|}{E_0} \right)^2 \right]^{-\frac{1}{2}} & \eta_1 = 2\eta_0 \end{cases} \quad (10)$$

where $E_0 > 0$, $\nu \in]-1, 1/2[$ and $\eta_0 > 0$ are the three parameters of the model. As for the previous model a nearly incompressible behaviour will be obtained by taking $\nu = 1/2 - \nu_\epsilon$ with small $\nu_\epsilon > 0$. Note that, eventually, the non-linear models given by equations (8), (9) and (10) are two particular forms of the more general one obtained from the constitutive equations (9) of Di Benedetto by replacing the previous expressions (10) of E and η by the following ones

$$\begin{cases} E(t) = E_1 \left[1 + \alpha_e \left(\frac{\|\mathbf{s}(t)\|}{E_0} \right)^{\beta_e} \right]^{\gamma_e} & E_1 = \frac{3}{2} E_0 \\ \eta(t) = \eta_1 \left[1 + \alpha_v \left(\frac{\|\mathbf{s}(t)\|}{E_0} \right)^{\beta_v} \right]^{-\gamma_v} & \eta_1 = 2\eta_0 \end{cases} \quad (11)$$

in which $\alpha_e, \beta_e, \gamma_e, \alpha_v, \beta_v$ and γ_v are six given positive constants. For concision's sake only this unified non-linear model defined by relations (9) and (11) will be considered in the rest of the paper.

3 Weak formulation of the time-discretized mechanical problem

Let $N \in \mathbb{N}^*$ and let t_0, t_1, \dots, t_N be an increasing sequence of time values, such that $t_0 = 0$ and $t_N = T$. In the following we are interested in the displacement fields $\mathbf{u}(t_n, \cdot)$ relating to the time values t_n , $n \in \{1, \dots, N\}$. We put, $\forall n \in \{0, \dots, N\}$ and $\forall x \in \Omega$, $\mathbf{u}_n(x) = \mathbf{u}(t_n, x)$, as well as analogous notations for $\sigma, \varepsilon, \mathbf{b}, \mathbf{g}$ and \mathbf{u}_i , and we denote as Δt_n the time increment $t_n - t_{n-1}$, $n \in \{1, \dots, N\}$. This section is devoted to the weak formulation of the time-discretized mechanical problem, whereas the following one focuses on the particularly important point constituted by the time discretization of the constitutive equations (6), (7), (9) and (11). The developments relating to this point which will be described below lead, for any given $n \in \{1, \dots, N\}$ and $x \in \Omega$, to the following formal relation

$$\varepsilon_n(x) = \mathbf{H}_{nx}(\sigma_n(x), \mathcal{H}_{nx}) \quad (12)$$

where \mathcal{H}_{nx} denotes the set of memory parameters different from $\sigma_n(x)$ at point x and at time t_n , including especially $\varepsilon_{n-1}(x)$ and $\sigma_{n-1}(x)$. The tensorial function \mathbf{H}_{nx} , which is always linear

with respect to $\sigma_n(x)$ if one considers the linear viscoelastic model given by relations (6) and (7), but which becomes non-linear when another scheme than a fully explicit one is chosen for the time discretization of the constitutive equations (9) and (11), is assumed to be one-to-one according to the principle of determinism. So we can write, formally,

$$\sigma_n(x) = \mathbf{H}_{nx}^{-1}(\varepsilon_n(x), \mathcal{H}_{nx}) \quad (13)$$

Let now $H^1(\Omega)$ be the Sobolev space of real square-integrable functions defined on Ω with square-integrable first-order generalized derivatives, and let $V = (H^1(\Omega))^3$. For any given $n \in \{1, \dots, N\}$ we denote as V_n the closed subspace of V of the functions $\mathbf{v} \in V$ such that $\mathbf{v}|_{\Gamma_1(t_n)} = 0$. Let us then consider the inner product of $\mathbf{v} \in V_n$ and the equation (2.1a) obtained for $t = t_n$ and integrate the resulting expression on Ω . Thus, after integration by parts and use of the Gauss integral identity, and taking into account the previous relation (13) together with the boundary conditions (2.3b) at time t_n , we obtain the classical weak formulation (\mathbf{P}_{nv}) of the time-discretized mechanical problem relating to time t_n

$$(\mathbf{P}_{nv}) \left\{ \begin{array}{l} \text{Find } \mathbf{u}_n \in V \text{ such that} \\ \int_{\Omega} \mathbf{H}_{nx}^{-1}(\varepsilon(\mathbf{u}_n), \mathcal{H}_{nx}) : \varepsilon(\mathbf{v}) d\Omega = \int_{\Omega} \mathbf{b}_n \cdot \mathbf{v} d\Omega + \int_{\Gamma_2(t_n)} \mathbf{g}_n \cdot \mathbf{v} d\Gamma \quad \forall \mathbf{v} \in V_n \\ \mathbf{u}_n = \mathbf{u}_{in} \text{ on } \Gamma_1(t_n) \end{array} \right. \quad (14)$$

where the operator ε is defined by $\varepsilon(\cdot) = (\mathbf{grad}_x(\cdot) + \mathbf{grad}_x^T(\cdot)) / 2$.

The variational problem (\mathbf{P}_{nv}) can then be solved by the finite element method after building a finite element space $V_h \subset V$. As mentioned above for (\mathbf{P}_{nv}) the problem (\mathbf{P}_{nh}) coming from the finite element space discretization remains always linear if one considers the linear viscoelastic model given by relations (6) and (7), but becomes non-linear when another scheme than a fully explicit one is chosen for the time discretization of the constitutive equations (9) and (11). Since in this last case the rheological non-linearities can increase greatly, the iterative resolution of (\mathbf{P}_{nh}) is carried out by using the robust Newton method. If $\mathbf{u}_n^{(r)}$ is the approximation coming from the resolution of the linearized problem ($\mathbf{P}_{nh}^{(r)}$) relating to the iteration (r), then ($\mathbf{P}_{nh}^{(r+1)}$) takes the following form

$$(\mathbf{P}_{nh}^{(r+1)}) \left\{ \begin{array}{l} \text{Find } \mathbf{u}_n^{(r+1)} \in V_h \text{ such that } \forall \mathbf{v} \in V_h \cap V_n \\ \int_{\Omega} \varepsilon(\mathbf{v}) : \mathbf{G}_{nx}^{-1}(\sigma_n^{(r)}, \mathcal{H}_{nx}) : \varepsilon(\mathbf{u}_n^{(r+1)}) d\Omega = \int_{\Gamma_2(t_n)} \mathbf{g}_n \cdot \mathbf{v} d\Gamma \\ \quad + \int_{\Omega} (\varepsilon(\mathbf{v}) : (\mathbf{G}_{nx}^{-1}(\sigma_n^{(r)}, \mathcal{H}_{nx}) : \mathbf{H}_{nx}(\sigma_n^{(r)}, \mathcal{H}_{nx}) - \sigma_n^{(r)}) + \mathbf{b}_n \cdot \mathbf{v}) d\Omega \\ \mathbf{u}_n^{(r+1)} = \mathbf{u}_{in} \text{ on } \Gamma_1(t_n) \end{array} \right. \quad (15)$$

where \mathbf{G}_{nx} is the gradient tensor of \mathbf{H}_{nx} . If, for simplicity's sake, we omit the subscripts n and x , then the components of the fourth-order tensor $\mathbf{G} = \mathbf{grad}_\sigma(\mathbf{H})$ are given by

$$\forall(i, j, k, l) \in \{1, 2, 3\}^4 \quad G_{ijkl} = \frac{\partial H_{ij}}{\partial \sigma_{kl}} \quad (16)$$

Finally the stop of iterations is governed by the following test

$$\left| \frac{\sigma_n^{(r+1)} - \sigma_n^{(r)}}{\sigma_n^{(r)}} \right| \leq e^{(tol)} \quad (17)$$

where $e^{(tol)}$ has a sufficient small value, for instance $e^{(tol)} = 10^{-6}$.

We shall now focus, in the following section, on the time discretization of the constitutive equations (6), (7), (9) and (11).

4 Time discretization of the constitutive equations

The present section is devoted to the time discretization of the constitutive equations given by (6), (7), (9) and (11). For that purpose three different time-discrete schemes, described below in three separate subsections, have been implemented in the finite element code ELFIM.⁸ In each of these subsections the principle of use of the corresponding scheme together with its accuracy order are first given by considering the following ordinary differential equation

$$\dot{v}(t) = f(v(t), u(t), \dot{u}(t)) \quad (18)$$

before applying the scheme considered to the time discretization of the previous constitutive equations. The real functions u and v of the real variable t which appear in the ordinary differential equation (18) above play analogous parts, respectively, to those of the tensorial functions σ and ε of the same variable t involved in the constitutive equations. However, some properties of the schemes studied, such as accuracy, but also, concerning one of them, its very principle of implementation, are strongly linked to the particular forms of such equations as (18) corresponding to the various viscoelastic bodies. So, in the following subsections, it will be necessary for us to resort to these particular forms. For instance let us note that the function f defining the differential equation (18) does not depend on v as concerns the various Maxwell one-dimensional bodies of the linear viscoelastic model, the constitutive equations of which are obtained from (3) by setting $M = 0$. We then get

$$\dot{v}(t) = f(u(t), \dot{u}(t)) = au(t) + b\dot{u}(t) \quad (19)$$

where the non-zero constants a and b have the same sign. This particularity holds also if one considers the unified non-linear viscoelastic model given by equations (9) and (11), for which we have

$$\dot{v}(t) = f(u(t), \dot{u}(t)) = a(u(t))u(t) + b(u(t))\dot{u}(t) \quad (20)$$

Finally f is dependent on v but not on \dot{u} as regards the constitutive relations (4) of the Kelvin-Voigt one-dimensional bodies involved in the linear viscoelastic model, for which we obtain

$$\dot{v}(t) = f(u(t), v(t)) = -av(t) + bu(t) \quad (21)$$

where a is a strictly positive constant.

In each of the corresponding subsections we shall also state the stability and superstability properties of the three schemes studied by considering the linear ordinary differential equation

$$\begin{cases} \dot{y}(t) = -\frac{y(t)}{\tau} & t > 0 \\ y(0) = y_0 \end{cases} \quad (22)$$

with given $\tau > 0$ and y_0 . Note that this equation can be obtained from (19) by setting $u = y$, $u(0) = y_0$, $ba^{-1} = \tau$ and $v(t) = v_0 \forall t \geq 0$, and also from (21) when $v = y$, $v(0) = y_0$, $a^{-1} = \tau$ and $u(t) = 0 \forall t > 0$. If one adopts a physical point of view, it corresponds in the first case to a relaxation test with a Maxwell body and in the second one to a recovery test with a Kelvin-Voigt body.

But to begin with we shall define both concepts of stability and superstability, in the first subsection and for the same equation (22), before illustrating them by considering two explicit Runge-Kutta schemes together with a non-explicit one.

4.1 Preliminary definitions

Let us consider the linear ordinary differential equation (22). In all this subsection we shall denote as Δt the time step $\Delta t_n = t_n - t_{n-1}$ (which is assumed to be constant for the sake of simplicity), as ρ the ratio $\rho = \Delta t/\tau$, and as (S) a given time-discrete scheme the use of which leads to the following numerical approximation y_n of $y(t_n)$

$$y_n = y_0 (\lambda(\rho))^n \quad n \in \mathbb{N}^* \quad (23)$$

We then have the

Definition 1 We say that the discrete approximation (23) is stable (resp. superstable) for a given $\rho > 0$ if $|\lambda(\rho)| \leq 1$ (resp. if $\lambda(\rho) \in [0, 1]$). Moreover, if the previous property holds $\forall \rho > 0$ we say that this approximation is unconditionally stable (resp. unconditionally superstable).

Let us now illustrate this definition by considering the classical fourth-order fully explicit Runge-Kutta scheme.¹² The principle of use of this scheme for the numerical resolution of the ordinary differential equation

$$\dot{y}(t) = f(y(t)) \quad (24)$$

is given by

$$\left\{ \begin{array}{l} y_{n,1} = y_n \\ y_{n,2} = y_n + \frac{h}{2}f(y_{n,1}) \\ y_{n,3} = y_n + \frac{h}{2}f(y_{n,2}) \\ y_{n,4} = y_n + hf(y_{n,3}) \\ y_{n+1} = y_n + \frac{h}{6}(f(y_{n,1}) + 2f(y_{n,2}) + 2f(y_{n,3}) + f(y_{n,4})) \end{array} \right. \quad (25)$$

and leads, as concerns equation (22), to approximation (23) with

$$\lambda(\rho) = 1 - \rho + \frac{\rho^2}{2} - \frac{\rho^3}{6} + \frac{\rho^4}{24} \quad (26)$$

The variations of the function $\rho \rightarrow \lambda(\rho)$ with $\rho > 0$ show that both stability and superstability are ensured as soon as $\rho \in]0, \rho_1]$ with $\rho_1 = \frac{2}{3} \left(2 + \sqrt[3]{\frac{43+9\sqrt{29}}{2}} + \sqrt[3]{\frac{43-9\sqrt{29}}{2}} \right)$ ($\rho_1 \approx 2.785294$).

By reconsidering the previous equation (24) the classical fifth-order fully explicit Runge-Kutta scheme (e.g. see Crouzeix¹³) is defined as follows

$$\left\{ \begin{array}{l} y_{n,1} = y_n \\ y_{n,2} = y_n + \frac{h}{2}f(y_{n,1}) \\ y_{n,3} = y_n + \frac{h}{16}(3f(y_{n,1}) + f(y_{n,2})) \\ y_{n,4} = y_n + \frac{h}{2}f(y_{n,3}) \\ y_{n,5} = y_n + \frac{h}{16}(-3f(y_{n,2}) + 6f(y_{n,3}) + 9f(y_{n,4})) \\ y_{n,6} = y_n + \frac{h}{7}(f(y_{n,1}) + 4f(y_{n,2}) + 6f(y_{n,3}) - 12f(y_{n,4}) + 8f(y_{n,5})) \\ y_{n+1} = y_n + \frac{h}{90}(7f(y_{n,1}) + 32f(y_{n,3}) + 12f(y_{n,4}) + 32f(y_{n,5}) + 7f(y_{n,6})) \end{array} \right. \quad (27)$$

and its use for solving equation (22) gives the approximation (23) with

$$\lambda(\rho) = 1 - \rho + \frac{\rho^2}{2} - \frac{\rho^3}{6} + \frac{\rho^4}{24} - \frac{\rho^5}{120} + \frac{\rho^6}{1280} \quad (28)$$

The study of the variations of this function with $\rho > 0$ shows that the stability requires $\rho \in]0, \rho_3]$ with $\rho_3 \approx 5.603972$, and that $\rho \in]0, \rho_1]$ with $\rho_1 \approx 2.629947$ or $\rho \in [\rho_2, \rho_3]$ with $\rho_2 \approx 5.116661$ is needed in order to obtain superstability.

Let us then deal with the non-explicit Runge-Kutta scheme known as Hammer and Hollingsworth method.¹⁴ When used for solving equation (24) this fourth-order scheme leads to

$$\begin{cases} y_{n,1} = y_n + \frac{h}{4} \left(f(y_{n,1}) + \left(1 - \frac{2}{\sqrt{3}}\right) f(y_{n,2}) \right) \\ y_{n,2} = y_n + \frac{h}{4} \left(\left(1 + \frac{2}{\sqrt{3}}\right) f(y_{n,1}) + f(y_{n,2}) \right) \\ y_{n+1} = y_n + \frac{h}{2} (f(y_{n,1}) + f(y_{n,2})) \end{cases} \quad (29)$$

and in the particular case of equation (22) we once more obtain the approximation (23) with the following expression of the function $\lambda(\rho)$

$$\lambda(\rho) = \frac{1 - \frac{\rho}{2} + \frac{\rho^2}{12}}{1 + \frac{\rho}{2} + \frac{\rho^2}{12}} \quad (30)$$

the variations of which (with $\rho > 0$) show that unconditional superstability is ensured.

Note that the previous results relating to the numerical approximation of equation (22) could have been anticipated. And indeed it is well known, for such kind of equation, that certain conditions are required in order to ensure the stability when fully explicit schemes are used, whereas unconditional stability can be obtained if one considers semi- or fully implicit ones. We shall now focus, in the three following subsections, on the three time-discrete schemes implemented in the finite element code ELFIM⁸ for the discretization of the constitutive equations given by (6), (7), (9) and (11). According to their order of implementation in the code these schemes will be denoted as S1, S2 and S3 in all the following,

4.2 The integral scheme S1

The first of those implemented in the finite element code ELFIM, the integral scheme S1 is based^{8,11} upon the following

Assumption 1 $\forall x \in \Omega$, the variations of the stresses $\sigma(t, x)$ are linear over each of the time intervals $[t_{n-1}, t_n]$, $n \in \{1, \dots, N\}$.

To begin with let us describe the principle of use of these scheme by considering the ordinary differential equation (18) together with its particular forms (19), (20) and (21) relating to the various viscoelastic bodies considered. The variations of the function $u(t)$ which plays, for given $x \in \Omega$, an analogous part to that of $\sigma(t, x)$, are assumed to be linear over each of the time intervals $[t_{n-1}, t_n]$, $n \in \{1, \dots, N\}$. So the approximations of u and \dot{u} resulting from this assumption, which have, respectively, $\mathcal{O}(\Delta t_n^2)$ and $\mathcal{O}(\Delta t_n)$ accuracy, lead to the following approximation of equation (18)

$$\dot{v}(t) = f \left(v(t), \frac{(t_n - t)u_{n-1} + (t - t_{n-1})u_n}{\Delta t_n}, \frac{u_n - u_{n-1}}{\Delta t_n} \right) \quad t \in]t_{n-1}, t_n[\quad (31)$$

Since the function f in equation (18) involves both u and \dot{u} , then the previous approximation (31) has $\mathcal{O}(\Delta t_n)$ accuracy, and the relation between v_n and u_n coming from its resolution has, on the face of it, $\mathcal{O}(\Delta t_n^2)$ accuracy. However we shall see in the following that this relation as a matter of fact has $\mathcal{O}(\Delta t_n^3)$ accuracy for the various viscoelastic bodies considered in this paper.

Let us first focus on the Kelvin-Voigt one-dimensional bodies involved in the linear viscoelastic model and given by relations (4). Then equation (18) takes the form (21) which does not depend on \dot{u} , and its approximation (31) becomes, with $\mathcal{O}(\Delta t_n^2)$ accuracy, as follows

$$\dot{v}(t) + av(t) = b \left(\frac{(t_n - t)u_{n-1} + (t - t_{n-1})u_n}{\Delta t_n}, \right) \quad t \in]t_{n-1}, t_n[\quad (32)$$

The exact resolution of this ordinary differential equation leads to the following relation binding v_n and u_n , with $\mathcal{O}(\Delta t_n^3)$ accuracy,

$$v_n = e^{-a\Delta t_n} v_{n-1} + \frac{b}{a} \left[\left(\frac{1 - e^{-a\Delta t_n}}{a\Delta t_n} - e^{-a\Delta t_n} \right) u_{n-1} + \left(1 - \frac{1 - e^{-a\Delta t_n}}{a\Delta t_n} \right) u_n \right] \quad (33)$$

Now if one considers the various Maxwell one-dimensional bodies of the same linear viscoelastic model, the constitutive equations of which are obtained from (3) by setting $M = 0$, together with the unified non-linear viscoelastic model given by equations (9) and (11), then equation (18) takes the form (19) or (20), respectively, and the function f becomes independent on v , so that (31) immediately gives

$$v_n - v_{n-1} = \int_{t_{n-1}}^{t_n} f \left(\frac{(t_n - t)u_{n-1} + (t - t_{n-1})u_n}{\Delta t_n}, \frac{u_n - u_{n-1}}{\Delta t_n} \right) dt \quad (34)$$

with, on the face of it, $\mathcal{O}(\Delta t_n^2)$ accuracy. However, the expression (19) of f relating to the linear Maxwell bodies shows that the previous relation leads to the exact integration of the

term $b\dot{u}(t)$, so that we get, for these linear models, $\mathcal{O}(\Delta t_n^3)$ accuracy. Its detailed expression, identical to that obtained by using the well-known Crank-Nicolson scheme (e.g. see [Crouzeix¹³](#)), is then as follows

$$v_n = v_{n-1} + \left(b + a \frac{\Delta t_n}{2}\right) u_n - \left(b - a \frac{\Delta t_n}{2}\right) u_{n-1} \quad (35)$$

Finally relation (34) has also $\mathcal{O}(\Delta t_n^3)$ accuracy as concerns the unified non-linear viscoelastic model, for which the function f is given by (20). And indeed we have, by considering this last relation, the following estimation of the error e in relation (34) coming from the approximation of the term $b(u(t)\dot{u}(t))$

$$\left\{ \begin{aligned} e &= \int_{t_{n-1}}^{t_n} \left[b(u(t)) \dot{u}(t) - b\left(\frac{(t_n - t)u_{n-1} + (t - t_{n-1})u_n}{\Delta t_n}\right) \frac{u_n - u_{n-1}}{\Delta t_n} \right] dt \\ &= \int_{t_{n-1}}^{t_n} b\left(\frac{(t_n - t)u_{n-1} + (t - t_{n-1})u_n}{\Delta t_n}\right) \left(\dot{u}(t) - \frac{u_n - u_{n-1}}{\Delta t_n}\right) dt + \mathcal{O}(\Delta t_n^3) \\ &= \int_{t_{n-1}}^{t_n} b(u_{n-1}) \left(\dot{u}(t) - \frac{u_n - u_{n-1}}{\Delta t_n}\right) dt + \mathcal{O}(\Delta t_n^3) \\ &= \mathcal{O}(\Delta t_n^3) \end{aligned} \right. \quad (36)$$

Now let us study the stability and superstability properties of scheme S1 when applied to the numerical resolution of equation (22). For that purpose the variations of the function $y(t)$ are assumed to be linear over each of the time intervals $[t_{n-1}, t_n]$, $n \in \{1, \dots, N\}$, and the time steps Δt_n are assumed to be constant for the sake of simplicity. So, after putting $\Delta t = \Delta t_n$ and $\rho = \Delta t/\tau$, we get the approximation (23) of $y(t_n)$ with

$$\lambda(\rho) = \frac{1 - \frac{\rho}{2}}{1 + \frac{\rho}{2}} \quad (37)$$

This approximation, which could be obtain from (35) by setting $u = y$, $u(0) = y_0$, $v(t) = v_0 \forall t \geq 0$ and $ba^{-1} = \tau$, is identical to the one coming from the Crank-Nicolson scheme, so that the unconditional stability is ensured whereas $\rho \in]0, 2]$ is required for superstability.

Now we shall focus on the time discretization of the constitutive equations given by (6), (7), (9) and (11). Let us first consider the linear viscoelastic model given by (6) and (7). Then, omitting the space variable x and taking into account relations (19), (21), (33) and (35) together with (6) and (7), the use of the scheme S1 for the time discretization of those constitutive equations leads to the following expression of the formal relation (12)

$$\varepsilon_n = \mathbf{H}_n(\sigma_n, \mathcal{H}_n) = \mathbf{M}_n : \sigma_n + \tilde{\varepsilon}_n \quad (38)$$

where the components of the fourth-order tensor \mathbf{M}_n together with those of the second-order tensor $\tilde{\varepsilon}_n$ are given^{8,11} by the following relations (39) and (40), respectively,

$$\left\{ \begin{array}{l} \forall (i, j, k, l) \in \{1, 2, 3\}^4 \text{ and without any summation on } i, j, k \text{ and } l : \\ M_{nijkl} = J_{ijkl}^{(0)} + \sum_{m=1}^{m=M} J_{ijkl}^{(m)} \left(1 - \frac{1 - e^{-\lambda_{ijkl}^{(m)} \Delta t_n}}{\lambda_{ijkl}^{(m)} \Delta t_n} \right) + J_{ijkl}^{(\infty)} \frac{\Delta t_n}{2} \end{array} \right. \quad (39)$$

$$\left\{ \begin{array}{l} \forall (i, j) \in \{1, 2, 3\}^2 \text{ and without any summation on } i \text{ and } j : \\ \tilde{\varepsilon}_{nij} = \varepsilon_{ij}(t_{n-1}) - \sum_{k=1}^{k=3} \sum_{l=1}^{l=3} \sum_{m=1}^{m=M} \left(1 - e^{-\lambda_{ijkl}^{(m)} \Delta t_n} \right) \varepsilon_{ijkl}^{(m)}(t_{n-1}) \\ + \sum_{k=1}^{k=3} \sum_{l=1}^{l=3} \sigma_{kl}(t_{n-1}) \left[-J_{ijkl}^{(0)} + \sum_{m=1}^{m=M} J_{ijkl}^{(m)} \left(\frac{1 - e^{-\lambda_{ijkl}^{(m)} \Delta t_n}}{\lambda_{ijkl}^{(m)} \Delta t_n} - e^{-\lambda_{ijkl}^{(m)} \Delta t_n} \right) + J_{ijkl}^{(\infty)} \frac{\Delta t_n}{2} \right] \end{array} \right. \quad (40)$$

The tensorial relation (38), which is linear with respect to σ_n , can then be inverted in order to obtain (13).

Now we are interested in the unified non-linear viscoelastic model, the constitutive equations of which are given by (9) and (11). Let then \mathbf{I}_4 be the fourth-order unit tensor and let \mathbf{C} and \mathbf{A} be the fourth-order tensors defined by

$$\mathbf{C} = \frac{-\nu}{E_1} \mathbf{I}_2 \otimes \mathbf{I}_2 + \frac{1+\nu}{E_1} \mathbf{I}_4 \quad \mathbf{A} = \frac{-1}{3} \mathbf{I}_2 \otimes \mathbf{I}_2 + \mathbf{I}_4 \quad (41)$$

So, taking into account relations (20) and (34) together with expressions (9) and (11), the formal relation (12) has the following form

$$\varepsilon_n = \mathbf{H}_n(\sigma_n, \mathcal{H}_n) = \left[I_1 \mathbf{C} + \frac{\Delta t_n}{\eta_1} I_3 \mathbf{A} \right] : (\sigma_n - \sigma_{n-1}) + \frac{\Delta t_n}{\eta_1} I_2 \mathbf{s}_{n-1} + \varepsilon_{n-1} \quad (42)$$

in which we have put, after setting $z = \frac{t - t_{n-1}}{\Delta t_n}$

$$\left\{ \begin{array}{l} I_1 = \int_0^1 \left[1 + \frac{\alpha_e}{E_0^{\beta_e}} (C_1 + C_2 z + C_3 z^2)^{\frac{\beta_e}{2}} \right]^{-\gamma_e} dz \\ I_2 = \int_0^1 \left[1 + \frac{\alpha_v}{E_0^{\beta_v}} (C_1 + C_2 z + C_3 z^2)^{\frac{\beta_v}{2}} \right]^{\gamma_v} dz \\ I_3 = \int_0^1 \left[1 + \frac{\alpha_v}{E_0^{\beta_v}} (C_1 + C_2 z + C_3 z^2)^{\frac{\beta_v}{2}} \right]^{\gamma_v} z dz \end{array} \right. \quad (43)$$

with

$$C_1 = \mathbf{s}_{n-1} : \mathbf{s}_{n-1} \quad C_2 = 2\mathbf{s}_{n-1} : (\mathbf{s}_n - \mathbf{s}_{n-1}) \quad C_3 = (\mathbf{s}_n - \mathbf{s}_{n-1}) : (\mathbf{s}_n - \mathbf{s}_{n-1}) \quad (44)$$

Since the tensorial relation (42) is non-linear with respect to σ_n , we need to exhibit the gradient \mathbf{G}_n of the non-linear tensorial function \mathbf{H}_n , the components of which are defined by (16). If one considers the linearized problem ($\mathbf{P}_{nh}^{(r+1)}$) relating to iteration $(r+1)$ and given by (15), then the gradient $\mathbf{G}_n^{(r)} = \mathbf{G}_n(\sigma_n^{(r)}, \mathcal{H}_n)$ is given by the following tensorial equality

$$\left\{ \begin{aligned} \mathbf{G}_n^{(r)} &= I_1^{(r)} \mathbf{C} + \frac{\Delta t_n}{\eta_1} I_3^{(r)} \mathbf{A} + [\mathbf{C} : (\sigma_n^{(r)} - \sigma_{n-1})] \otimes [(I_{12}^{(r)} - I_{13}^{(r)}) \mathbf{s}_{n-1} + I_{13}^{(r)} \mathbf{s}_n^{(r)}] \\ &+ \frac{\Delta t_n}{\eta_1} [(I_{22}^{(r)} - 2I_{23}^{(r)} + I_{33}^{(r)}) \mathbf{s}_{n-1} \otimes \mathbf{s}_{n-1} + I_{33}^{(r)} \mathbf{s}_n^{(r)} \otimes \mathbf{s}_n^{(r)}] \\ &+ \frac{\Delta t_n}{\eta_1} (I_{23}^{(r)} - I_{33}^{(r)}) [\mathbf{s}_{n-1} \otimes \mathbf{s}_n^{(r)} + \mathbf{s}_n^{(r)} \otimes \mathbf{s}_{n-1}] \end{aligned} \right. \quad (45)$$

with

$$\left\{ \begin{aligned} I_{12}^{(r)} &= \frac{-\alpha_e \beta_e \gamma_e}{E_0^{\beta_e}} \int_0^1 \left[1 + \frac{\alpha_e}{E_0^{\beta_e}} (g^{(r)}(z))^{\frac{\beta_e}{2}} \right]^{-\gamma_e - 1} (g^{(r)}(z))^{\frac{\beta_e}{2} - 1} z dz \\ I_{13}^{(r)} &= \frac{-\alpha_e \beta_e \gamma_e}{E_0^{\beta_e}} \int_0^1 \left[1 + \frac{\alpha_e}{E_0^{\beta_e}} (g^{(r)}(z))^{\frac{\beta_e}{2}} \right]^{-\gamma_e - 1} (g^{(r)}(z))^{\frac{\beta_e}{2} - 1} z^2 dz \\ I_{22}^{(r)} &= \frac{\alpha_v \beta_v \gamma_v}{E_0^{\beta_v}} \int_0^1 \left[1 + \frac{\alpha_v}{E_0^{\beta_v}} (g^{(r)}(z))^{\frac{\beta_v}{2}} \right]^{\gamma_v - 1} (g^{(r)}(z))^{\frac{\beta_v}{2} - 1} z dz \\ I_{23}^{(r)} &= \frac{\alpha_v \beta_v \gamma_v}{E_0^{\beta_v}} \int_0^1 \left[1 + \frac{\alpha_v}{E_0^{\beta_v}} (g^{(r)}(z))^{\frac{\beta_v}{2}} \right]^{\gamma_v - 1} (g^{(r)}(z))^{\frac{\beta_v}{2} - 1} z^2 dz \\ I_{33}^{(r)} &= \frac{\alpha_v \beta_v \gamma_v}{E_0^{\beta_v}} \int_0^1 \left[1 + \frac{\alpha_v}{E_0^{\beta_v}} (g^{(r)}(z))^{\frac{\beta_v}{2}} \right]^{\gamma_v - 1} (g^{(r)}(z))^{\frac{\beta_v}{2} - 1} z^3 dz \end{aligned} \right. \quad (46)$$

where the function $g^{(r)}(z)$ is defined by

$$g^{(r)}(z) = C_1 + C_2^{(r)} z + C_3^{(r)} z^2 \quad \forall z \in [0, 1] \quad (47)$$

The subscript (r) attached to the above-defined scalar quantities such as I_1, I_{12}, C_2, \dots , means that their evaluation is made by using the value $\mathbf{s}_n^{(r)}$ of \mathbf{s}_n coming from the resolution of the linearized problem ($\mathbf{P}_{nh}^{(r)}$) relating to the previous iteration (r) .

Let us finally point out that relations (42),(43), (45) and (46) above have been established by considering the unified non-linear viscoelastic model given by equations (9) and (11). These expressions become simplified if one considers the initial model given by equations (9) and (10), and more particularly the modified Maxwell-Norton-Hoff model given by equation (8), the elastic part of which remains linear. The simplified expressions corresponding to these two models can be found in Royis.¹⁵

4.3 The θ -scheme S2

The classical θ -scheme (e.g. see Crouzeix¹³), denoted as S2 in the following, is the second of those implemented in the finite element code ELFIM. Its implementation was made in order to analyse and compare the accuracy of numerical solutions of finite element computations obtained by using both schemes S1 and S2.¹⁶ The principle of use of the θ -scheme S2, which consists in a linear combination (depending on the parameter $\theta \in [0, 1]$) of the fully explicit and fully implicit Euler schemes, can be easily described if one considers the ordinary differential equation (18), for which it leads to the following approximation

$$v_n = v_{n-1} + \Delta t_n \left[(1 - \theta) f \left(v_{n-1}, u_{n-1}, \frac{u_n - u_{n-1}}{\Delta t_n} \right) + \theta f \left(v_n, u_n, \frac{u_n - u_{n-1}}{\Delta t_n} \right) \right] \quad (48)$$

If $\theta = 0$ we get the fully explicit Euler scheme, if $\theta = 1$ the fully implicit one and if $\theta = 1/2$ the Crank-Nicolson scheme. It is well known that scheme S2 has $\mathcal{O}(\Delta t_n^2)$ accuracy if $\theta = 1/2$, and $\mathcal{O}(\Delta t_n)$ accuracy if not. In other terms the previous approximation (48) has $\mathcal{O}(\Delta t_n^3)$ accuracy if $\theta = 1/2$, and $\mathcal{O}(\Delta t_n^2)$ accuracy if not.

On the other hand the use of scheme S2 for the numerical resolution of equation (22) gives, if one considers constant time steps $\Delta t_n = \Delta t$ and after setting $\rho = \Delta t/\tau$, the approximation (23) of $y(t_n)$ with

$$\lambda(\rho) = \frac{1 - (1 - \theta)\rho}{1 + \theta\rho} \quad (49)$$

The study of the variations of the previous function $\rho \rightarrow \lambda(\rho)$ with $\rho > 0$ shows that the stability is unconditional if $\theta \in [1/2, 1]$, and that the following condition $\rho \in]0, \frac{2}{1-2\theta}]$ is needed if $\theta \in [0, 1/2[$. It shows also that the superstability is unconditional only when $\theta = 1$, whereas the condition $\rho \in]0, \frac{1}{1-\theta}]$ is required if $\theta \in [0, 1[$.

If we now have a second look at the linear viscoelastic model the constitutive equations of which are given by (6) and (7), then the θ -scheme S2 like S1 leads to the relation (38). The components of the fourth-order tensor \mathbf{M}_n , together with those of the second-order tensor $\tilde{\varepsilon}_n$ defining this relation, are given by the following expressions (50) and (51), respectively,

$$\left\{ \begin{array}{l} \forall (i, j, k, l) \in \{1, 2, 3\}^4 \text{ and without any summation on } i, j, k \text{ and } l : \\ M_{nijkl} = J_{ijkl}^{(0)} + \theta \Delta t_n \left[\sum_{m=1}^{m=M} \frac{1}{\eta_{ijkl}^{(m)} (1 + \theta \lambda_{ijkl}^{(m)} \Delta t_n)} + J_{ijkl}^{(\infty)} \right] \end{array} \right. \quad (50)$$

$$\left\{ \begin{array}{l} \forall (i, j) \in \{1, 2, 3\}^2 \text{ and without any summation on } i \text{ and } j : \\ \tilde{\varepsilon}_{nij} = \varepsilon_{ij}(t_{n-1}) - \Delta t_n \sum_{k=1}^{k=3} \sum_{l=1}^{l=3} \sum_{m=1}^{m=M} \frac{\lambda_{ijkl}^{(m)}}{1 + \theta \lambda_{ijkl}^{(m)} \Delta t_n} \varepsilon_{ijkl}^{(m)}(t_{n-1}) \\ + \sum_{k=1}^{k=3} \sum_{l=1}^{l=3} \sigma_{kl}(t_{n-1}) \left[-J_{ijkl}^{(0)} + (1 - \theta) \Delta t_n \left(\sum_{m=1}^{m=M} \frac{1}{\eta_{ijkl}^{(m)} (1 + \theta \lambda_{ijkl}^{(m)} \Delta t_n)} + J_{ijkl}^{(\infty)} \right) \right] \end{array} \right. \quad (51)$$

and the corresponding tensorial relation, which as in the previous subsection remains linear with respect to σ_n , can be easily inverted in order to obtain (13).

As to the unified non-linear viscoelastic model defined by equations (9) and (11), the use of scheme S2 gives the following expression of the formal relation (12)

$$\left\{ \begin{array}{l} \varepsilon_n = \mathbf{H}_n(\sigma_n, \mathcal{H}_n) \\ = [\theta I_1 + (1 - \theta) I_0] \mathbf{C} : (\sigma_n - \sigma_{n-1}) + \frac{\Delta t_n}{\eta_1} [\theta J_1 \mathbf{s}_n + (1 - \theta) J_0 \mathbf{s}_{n-1}] + \varepsilon_{n-1} \end{array} \right. \quad (52)$$

in which \mathbf{C} is defined by (41), whereas I_0 , I_1 , J_0 and J_1 are given by the following expressions

$$\left\{ \begin{array}{l} I_0 = \left[1 + \alpha_e \left(\frac{\|\mathbf{s}_{n-1}\|}{E_0} \right)^{\beta_e} \right]^{-\gamma_e} \\ J_0 = \left[1 + \alpha_v \left(\frac{\|\mathbf{s}_{n-1}\|}{E_0} \right)^{\beta_v} \right]^{\gamma_v} \end{array} \right. \quad \left\{ \begin{array}{l} I_1 = \left[1 + \alpha_e \left(\frac{\|\mathbf{s}_n\|}{E_0} \right)^{\beta_e} \right]^{-\gamma_e} \\ J_1 = \left[1 + \alpha_v \left(\frac{\|\mathbf{s}_n\|}{E_0} \right)^{\beta_v} \right]^{\gamma_v} \end{array} \right. \quad (53)$$

Since the tensorial relation (52) becomes non-linear with respect to σ_n as soon as $\theta \neq 0$, we have, as in the previous subsection for scheme S1, to compute the fourth-order gradient tensor $\mathbf{G}_n^{(r)} = \mathbf{G}_n(\sigma_n^{(r)}, \mathcal{H}_n)$ required by the numerical resolution of the linearized problem ($\mathbf{P}_{nh}^{(r+1)}$) given by (15) and relating to iteration $(r + 1)$. Its expression is as follows

$$\left\{ \begin{array}{l} \mathbf{G}_n^{(r)} = [\theta I_1^{(r)} + (1 - \theta) I_0] \mathbf{C} \\ + \theta \left[I_{12}^{(r)} [\mathbf{C} : (\sigma_n^{(r)} - \sigma_{n-1})] \otimes \mathbf{s}_n^{(r)} + \frac{\Delta t_n}{\eta_1} (J_1^{(r)} \mathbf{A} + J_{12}^{(r)} \mathbf{s}_n^{(r)} \otimes \mathbf{s}_n^{(r)}) \right] \end{array} \right. \quad (54)$$

where the fourth-order tensor \mathbf{A} is defined by (41), whereas $I_{12}^{(r)}$ and $J_{12}^{(r)}$ are given by

$$\left\{ \begin{array}{l} I_{12}^{(r)} = \frac{-\alpha_e \beta_e \gamma_e}{E_0^{\beta_e}} \|\mathbf{s}_n^{(r)}\|^{\beta_e - 2} \left[1 + \alpha_e \left(\frac{\|\mathbf{s}_n^{(r)}\|}{E_0} \right)^{\beta_e} \right]^{-\gamma_e - 1} \\ J_{12}^{(r)} = \frac{\alpha_v \beta_v \gamma_v}{E_0^{\beta_v}} \|\mathbf{s}_n^{(r)}\|^{\beta_v - 2} \left[1 + \alpha_v \left(\frac{\|\mathbf{s}_n^{(r)}\|}{E_0} \right)^{\beta_v} \right]^{\gamma_v - 1} \end{array} \right. \quad (55)$$

Let us remind the reader that the subscript (r) attached to any given scalar quantity means that its evaluation is made by using the value $\mathbf{s}_n^{(r)}$ of \mathbf{s}_n coming from the resolution of the linearized problem ($\mathbf{P}_{nh}^{(r)}$) relating to the previous iteration (r) .

On the other hand, it is obvious that the previous relations (52), (53), (54) and (55), which have been established by considering the unified non-linear viscoelastic model given by equations (9) and (11), become simplified if one considers the two initial models given by equations (8), (9) and (10). These simplified expressions can be found in Royis.¹⁵

4.4 The scheme S3

To begin with, let us explain, as in the two previous subsections, the principle of use of these original scheme by considering the ordinary differential equation (18) together with its particular forms (19), (20) and (21) relating to the various viscoelastic bodies considered.

In order to ensure both unconditional stability and $\mathcal{O}(\Delta t_n^2)$ accuracy of scheme S3 we start with a backward $\mathcal{O}(\Delta t_n^3)$ -accurate Taylor series expansion of v_{n-1} , $n \in \{1, \dots, N\}$, as follows

$$v_{n-1} = v_n - \Delta t_n \dot{v}_n + \frac{\Delta t_n^2}{2} \ddot{v}_n + \mathcal{O}(\Delta t_n^3) \quad (56)$$

and then we replace \dot{v}_n by its expressions coming from (18), and \ddot{v}_n by the total time derivative of the same expression. If we choose to denote as $\frac{D}{Dt}$ the operator of total time derivation, we then get

$$v_{n-1} = v_n - \Delta t_n f(v_n, u_n, \dot{u}_n) + \frac{\Delta t_n^2}{2} \frac{D}{Dt} f(v_n, u_n, \dot{u}_n) + \mathcal{O}(\Delta t_n^3) \quad (57)$$

We still have to obtain a first-order approximation of the total time derivative $\frac{Df}{Dt}$ of f . The simplest way of doing this consists in using the first-order backward Euler scheme. Unfortunately this amounts to work with the Crank-Nicolson scheme (i.e. the θ -scheme S2 with $\theta = 1/2$), and that is the reason why we shall try, in the following, to perform this approximation on the basis of a total time derivation of f . Consequently, the bringing into play of the scheme described in this subsection is strongly linked, as shown in the following paragraphs, to the particular forms (19), (20) and (21) of the equation (18) corresponding to the various viscoelastic bodies considered.

To begin with let us consider the Kelvin-Voigt one-dimensional bodies involved in the linear viscoelastic model and given by relations (4), for which f takes the form (21). When putting this expression together with its time derivative in relation (57) we get

$$v_{n-1} = v_n - \Delta t_n (-av_n + bu_n) + \frac{\Delta t_n^2}{2} (-a\dot{v}_n + b\dot{u}_n) + \mathcal{O}(\Delta t_n^3) \quad (58)$$

and by using (21) again in order to express \dot{v}_n we have

$$\left\{ \begin{aligned} v_{n-1} &= v_n - \Delta t_n(-av_n + bu_n) + \frac{\Delta t_n^2}{2}(-a(-av_n + bu_n) + b\dot{u}_n) + \mathcal{O}(\Delta t_n^3) \\ &= \left(1 + a\Delta t_n + \frac{(a\Delta t_n)^2}{2}\right)v_n - b\Delta t_n\left(1 + \frac{a\Delta t_n}{2}\right)u_n \\ &\quad + \frac{b\Delta t_n^2}{2}\left(\frac{u_n - u_{n-1}}{\Delta t_n} + \mathcal{O}(\Delta t_n)\right) + \mathcal{O}(\Delta t_n^3) \\ &= \left(1 + a\Delta t_n + \frac{(a\Delta t_n)^2}{2}\right)v_n - \frac{b\Delta t_n}{2}u_{n-1} - \frac{b\Delta t_n}{2}(1 + a\Delta t_n)u_n + \mathcal{O}(\Delta t_n^3) \end{aligned} \right. \quad (59)$$

so that we get, for the models considered, the following $\mathcal{O}(\Delta t_n^3)$ -accurate approximation

$$v_n = \frac{b\Delta t_n(1 + a\Delta t_n)u_n + b\Delta t_n u_{n-1} + 2v_{n-1}}{1 + (1 + a\Delta t_n)^2} \quad (60)$$

Let us now deal with the various Maxwell one-dimensional bodies of the same linear viscoelastic model, the constitutive equations of which are obtained from (3) by setting $M = 0$, and for which equation (18) takes the form (19), and let us adopt the previous approach. We then get

$$\left\{ \begin{aligned} v_{n-1} &= v_n - \Delta t_n(au_n + b\dot{u}_n) + \frac{\Delta t_n^2}{2}(a\dot{u}_n + b\ddot{u}_n) + \mathcal{O}(\Delta t_n^3) \\ &= v_n - a\Delta t_n u_n + b\left(-\Delta t_n \dot{u}_n + \frac{\Delta t_n^2}{2}\ddot{u}_n\right) \\ &\quad + \frac{a\Delta t_n^2}{2}\left(\frac{u_n - u_{n-1}}{\Delta t_n} + \mathcal{O}(\Delta t_n)\right) + \mathcal{O}(\Delta t_n^3) \\ &= v_n - a\Delta t_n u_n + b(u_{n-1} - u_n + \mathcal{O}(\Delta t_n^3)) + \frac{a\Delta t_n}{2}(u_n - u_{n-1}) + \mathcal{O}(\Delta t_n^3) \\ &= v_n + \left(b - \frac{a\Delta t_n}{2}\right)u_{n-1} - \left(b + \frac{a\Delta t_n}{2}\right)u_n + \mathcal{O}(\Delta t_n^3) \end{aligned} \right. \quad (61)$$

and we can observe that the resulting $\mathcal{O}(\Delta t_n^3)$ -accurate approximation is identical to the one given by (35) coming from the integral scheme S1, which, for the linear viscoelastic bodies considered, coincides with the approximation coming from the Crank-Nicolson scheme. This is due to the fact that in this case the expression (19) of the function f does not depend on v anymore. So we need, in order to obtain an original approximation like the (60) one, to swap the parts of u and v , that is to say, to start with a backward $\mathcal{O}(\Delta t_n^3)$ -accurate Taylor series expansion of u_{n-1} , $n \in \{1, \dots, N\}$,

$$u_{n-1} = u_n - \Delta t_n \dot{u}_n + \frac{\Delta t_n^2}{2}\ddot{u}_n + \mathcal{O}(\Delta t_n^3) \quad (62)$$

That is in this sense that the bringing into play of the scheme developed in this subsection is strongly linked to the particular form of the constitutive equations considered. We then

obtain, after replacing in (62) \dot{u}_n and \ddot{u}_n by their expressions coming from (19) and from the time derivative of this same relation,

$$u_{n-1} = u_n - \frac{\Delta t_n}{b}(-au_n + \dot{v}_n) + \frac{\Delta t_n^2}{2b}(-a\dot{u}_n + \ddot{v}_n) + \mathcal{O}(\Delta t_n^3) \quad (63)$$

and by using (19) again in order to express \dot{u}_n we have

$$\left\{ \begin{aligned} u_{n-1} &= u_n - \frac{\Delta t_n}{b}(-au_n + \dot{v}_n) + \frac{\Delta t_n^2}{2b} \left(-\frac{a}{b}(-au_n + \dot{v}_n) + \ddot{v}_n \right) + \mathcal{O}(\Delta t_n^3) \\ &= \left(1 + \frac{a\Delta t_n}{b} + \frac{1}{2} \left(\frac{a\Delta t_n}{b} \right)^2 \right) u_n + \frac{1}{b} \left(-\Delta t_n \dot{v}_n + \frac{\Delta t_n^2}{2} \ddot{v}_n \right) \\ &\quad - \frac{a}{2} \left(\frac{\Delta t_n}{b} \right)^2 \dot{v}_n + \mathcal{O}(\Delta t_n^3) \\ &= \left(1 + \frac{a\Delta t_n}{b} + \frac{1}{2} \left(\frac{a\Delta t_n}{b} \right)^2 \right) u_n + \frac{1}{b} (v_{n-1} - v_n + \mathcal{O}(\Delta t_n^3)) \\ &\quad - \frac{a}{2} \left(\frac{\Delta t_n}{b} \right)^2 \left(\frac{v_n - v_{n-1}}{\Delta t_n} + \mathcal{O}(\Delta t_n) \right) + \mathcal{O}(\Delta t_n^3) \\ &= \left(1 + \frac{a\Delta t_n}{b} + \frac{1}{2} \left(\frac{a\Delta t_n}{b} \right)^2 \right) u_n + \frac{1}{b} \left(1 + \frac{a\Delta t_n}{2b} \right) (v_{n-1} - v_n) + \mathcal{O}(\Delta t_n^3) \end{aligned} \right. \quad (64)$$

We then get, for the linear viscoelastic bodies considered, the following $\mathcal{O}(\Delta t_n^3)$ -accurate approximation

$$v_n = v_{n-1} + \frac{\left(2b + 2a\Delta t_n + \frac{(a\Delta t_n)^2}{b} \right) u_n - 2bu_{n-1}}{2 + \frac{a\Delta t_n}{b}} \quad (65)$$

Finally let us consider the unified non-linear viscoelastic model given by equations (9) and (11), for which equation (18) takes the form (20). In the following, for the sake of simplicity and $\forall n \in \{0, \dots, N\}$, we shall put $a_n = a(u_n)$, $b_n = b(u_n)$, $\dot{a}_n = \frac{D}{Dt}a(u_n)$ and $\dot{b}_n = \frac{D}{Dt}b(u_n)$. So, by starting in the same way as for the previous Maxwell one-dimensional bodies we obtain the following relation

$$\left\{ \begin{aligned} u_{n-1} &= u_n - \frac{\Delta t_n}{b_n}(-a_n u_n + \dot{v}_n) + \frac{\Delta t_n^2}{2b_n}(-a_n \dot{u}_n + \ddot{v}_n) \\ &\quad - \frac{\Delta t_n^2}{2b_n} \left(\dot{a}_n u_n + \frac{\dot{b}_n}{b_n}(-a_n u_n + \dot{v}_n) \right) + \mathcal{O}(\Delta t_n^3) \end{aligned} \right. \quad (66)$$

in which the last term, induced by the non-linear nature of equation (20), can be approximated in a simple way as follows

$$\left\{ \begin{aligned} \dot{a}_n u_n + \frac{\dot{b}_n}{b_n}(-a_n u_n + \dot{v}_n) &= \dot{a}_n u_n + \dot{b}_n \dot{u}_n \\ &= \frac{a_n - a_{n-1}}{\Delta t_n} u_n + \frac{b_n - b_{n-1}}{\Delta t_n} \frac{u_n - u_{n-1}}{\Delta t_n} + \mathcal{O}(\Delta t_n) \end{aligned} \right. \quad (67)$$

Then, from (66) and (67) and by proceeding as in the relations (64) above, we have

$$\begin{cases} u_{n-1} = \left(1 + \frac{a_n \Delta t_n}{b_n} + \frac{1}{2} \left(\frac{a_n \Delta t_n}{b_n}\right)^2\right) u_n + \frac{1}{b_n} \left(1 + \frac{a_n \Delta t_n}{2b_n}\right) (v_{n-1} - v_n) \\ - \frac{\Delta t_n}{2b_n} (a_n - a_{n-1}) u_n - \frac{b_n - b_{n-1}}{2b_n} (u_n - u_{n-1}) + \mathcal{O}(\Delta t_n^3) \end{cases} \quad (68)$$

which leads to the following $\mathcal{O}(\Delta t_n^3)$ -accurate approximation

$$v_n = v_{n-1} + \frac{\left(b_n + b_{n-1} + \Delta t_n (a_n + a_{n-1}) + \frac{(a_n \Delta t_n)^2}{b_n}\right) u_n - (b_n + b_{n-1}) u_{n-1}}{2 + \frac{a_n \Delta t_n}{b_n}} \quad (69)$$

As in the two previous subsections we study the stability and superstability properties of scheme S3 when applied to the numerical resolution of equation (22). By considering constant time steps $\Delta t_n = \Delta t$ and after putting $\rho = \Delta t/\tau$ we once more get the approximation (23) of $y(t_n)$, with the following expression of the function $\lambda(\rho)$

$$\lambda(\rho) = \frac{1}{1 + \rho + \frac{\rho^2}{2}} \quad (70)$$

This expression, which could be obtained from (65) by setting $u = y$, $u(0) = y_0$, $v(t) = v_0 \forall t \geq 0$ and $ba^{-1} = \tau$, shows that the unconditional superstability holds.

Let us now apply scheme S3 to the time discretization of the constitutive equations (6) and (7) relating to the linear viscoelastic model. As for the schemes S1 and S2 previously described the use of scheme S3 leads to the tensorial relation (38), and the components of the fourth-order tensor \mathbf{M}_n together with those of the second-order tensor $\tilde{\varepsilon}_n$ defining this relation are given, taking into account relations (19), (21), (65), (60) together with (6) and (7), by the following expressions (71) and (72), respectively,

$$\begin{cases} \forall (i, j, k, l) \in \{1, 2, 3\}^4 \text{ and without any summation on } i, j, k \text{ and } l : \\ M_{nijkl} = J_{ijkl}^{(0)} + \Delta t_n \left[\sum_{m=1}^{m=M} \frac{1}{\eta_{ijkl}^{(m)}} \frac{1 + \lambda_{ijkl}^{(m)} \Delta t_n}{1 + \left(1 + \lambda_{ijkl}^{(m)} \Delta t_n\right)^2} + J_{ijkl}^{(\infty)} \frac{J_{ijkl}^{(0)} + J_{ijkl}^{(\infty)} \Delta t_n}{2J_{ijkl}^{(0)} + J_{ijkl}^{(\infty)} \Delta t_n} \right] \end{cases} \quad (71)$$

$$\begin{cases} \forall (i, j) \in \{1, 2, 3\}^2 \text{ and without any summation on } i \text{ and } j : \\ \tilde{\varepsilon}_{nij} = \varepsilon_{ij}(t_{n-1}) - \Delta t_n \sum_{k=1}^{k=3} \sum_{l=1}^{l=3} \sum_{m=1}^{m=M} \lambda_{ijkl}^{(m)} \frac{2 + \lambda_{ijkl}^{(m)} \Delta t_n}{1 + \left(1 + \lambda_{ijkl}^{(m)} \Delta t_n\right)^2} \varepsilon_{ijkl}^{(m)}(t_{n-1}) \\ + \sum_{k=1}^{k=3} \sum_{l=1}^{l=3} \sigma_{kl}(t_{n-1}) \left[\Delta t_n \sum_{m=1}^{m=M} \frac{1}{\eta_{ijkl}^{(m)}} \frac{1}{1 + \left(1 + \lambda_{ijkl}^{(m)} \Delta t_n\right)^2} - \frac{2J_{ijkl}^{(0)} J_{ijkl}^{(0)}}{2J_{ijkl}^{(0)} + J_{ijkl}^{(\infty)} \Delta t_n} \right] \end{cases} \quad (72)$$

If one now considers the unified non-linear viscoelastic model, the constitutive equations of which are given by (9) and (11), then the formal relation (12) takes, when using scheme S3 and taking into account relations (20) and (69) together with expressions (9) and (11), the following form

$$\varepsilon_n = \mathbf{H}_n(\sigma_n, \mathcal{H}_n) = \frac{I_0 + I_1}{2} \mathbf{C} : (\sigma_n - \sigma_{n-1}) + \frac{\Delta t_n}{\eta_1} [A_1 \mathbf{s}_n + A_2 \mathbf{s}_{n-1}] + \varepsilon_{n-1} \quad (73)$$

with

$$A_1 = \frac{J_0 + \frac{I_1 - I_0}{2I_1} J_1 + \frac{\Delta t_n}{\eta_1} \frac{E_1}{1 + \nu} \frac{J_1^2}{I_1}}{2 + \frac{\Delta t_n}{\eta_1} \frac{E_1}{1 + \nu} \frac{J_1}{I_1}} \quad A_2 = \frac{\frac{I_0 + I_1}{2I_1} J_1}{2 + \frac{\Delta t_n}{\eta_1} \frac{E_1}{1 + \nu} \frac{J_1}{I_1}} \quad (74)$$

where \mathbf{C} is defined by (41), whereas I_0 , I_1 , J_0 and J_1 are given by (53). The starting point for the statement of the previous expression of \mathbf{H}_n is given by the following tensorial equality which can be easily obtained, taking into account the definition (41) of \mathbf{A} , from relations (9), (11), (20) and (68).

$$\left\{ \begin{array}{l} \frac{I_0 + I_1}{2I_1} (\sigma_{n-1} - \sigma_n) = \left[\frac{\Delta t_n}{\eta_1} \frac{J_0 + J_1}{2I_1} \mathbf{C}^{-1} : \mathbf{A} + \frac{1}{2} \left(\frac{\Delta t_n}{\eta_1} \frac{J_1}{I_1} \right)^2 \mathbf{C}^{-1} : \mathbf{A} : \mathbf{C}^{-1} : \mathbf{A} \right] : \sigma_n \\ - \frac{1}{I_1} \mathbf{C}^{-1} : \left[\mathbf{I}_4 + \frac{1}{2} \frac{\Delta t_n}{\eta_1} \frac{J_1}{I_1} \mathbf{A} : \mathbf{C}^{-1} \right] : (\varepsilon_n - \varepsilon_{n-1}) \end{array} \right. \quad (75)$$

The expression of the tensorial function \mathbf{H}_n given by (73) and (74) then ensues from the following properties of the fourth-order tensors \mathbf{A} and \mathbf{C}

$$\left\{ \begin{array}{l} (\mathbf{I}_4 + a\mathbf{A})^{-1} = \mathbf{I}_4 - \frac{a}{a+1} \mathbf{A} \quad \forall a \neq -1 \quad \mathbf{A} : \mathbf{A} = \mathbf{A} \\ \mathbf{C}^{-1} : \mathbf{A} = \mathbf{A} : \mathbf{C}^{-1} = \frac{E_1}{1 + \nu} \mathbf{A} \quad \mathbf{C} : \mathbf{A} = \mathbf{A} : \mathbf{C} = \frac{1 + \nu}{E_1} \mathbf{A} \end{array} \right. \quad (76)$$

As in the two previous subsections this function is non-linear with respect to σ_n , so that we need to exhibit the fourth-order gradient tensor $\mathbf{G}_n^{(r)} = \mathbf{G}_n(\sigma_n^{(r)}, \mathcal{H}_n)$ required for the numerical resolution of the linearized problem ($\mathbf{P}_{nh}^{(r+1)}$) given by (15) and relating to iteration $(r+1)$. We finally obtain

$$\left\{ \begin{array}{l} \mathbf{G}_n^{(r)} = \frac{I_0 + I_1^{(r)}}{2} \mathbf{C} + \frac{I_{12}^{(r)}}{2} [\mathbf{C} : (\sigma_n^{(r)} - \sigma_{n-1})] \otimes \mathbf{s}_n^{(r)} \\ + \frac{\Delta t_n}{\eta_1} [A_1^{(r)} \mathbf{A} + (G_1^{(r)} \mathbf{s}_n^{(r)} + G_2^{(r)} \mathbf{s}_{n-1}) \otimes \mathbf{s}_n^{(r)}] \end{array} \right. \quad (77)$$

with

$$G_1^{(r)} = I_{12}^{(r)} \frac{\frac{I_0 J_1^{(r)}}{(I_1^{(r)})^2} + \frac{\Delta t_n}{\eta_1} \frac{E_1}{1 + \nu} \frac{J_1^{(r)}}{I_1^{(r)}} \frac{2J_0 - 3J_1^{(r)}}{2I_1^{(r)}}}{\left(2 + \frac{\Delta t_n}{\eta_1} \frac{E_1}{1 + \nu} \frac{J_1^{(r)}}{I_1^{(r)}}\right)^2} + J_{12}^{(r)} \frac{\frac{I_1^{(r)} - I_0}{I_1^{(r)}} + \frac{\Delta t_n}{\eta_1} \frac{E_1}{1 + \nu} \frac{4J_1^{(r)} - J_0}{I_1^{(r)}} + \left(\frac{\Delta t_n}{\eta_1} \frac{E_1}{1 + \nu} \frac{J_1^{(r)}}{I_1^{(r)}}\right)^2}{\left(2 + \frac{\Delta t_n}{\eta_1} \frac{E_1}{1 + \nu} \frac{J_1^{(r)}}{I_1^{(r)}}\right)^2} \quad (78)$$

and

$$G_2^{(r)} = I_{12}^{(r)} \frac{-\frac{I_0 J_1^{(r)}}{(I_1^{(r)})^2} + \frac{\Delta t_n}{2\eta_1} \frac{E_1}{1 + \nu} \left(\frac{J_1^{(r)}}{I_1^{(r)}}\right)^2}{\left(2 + \frac{\Delta t_n}{\eta_1} \frac{E_1}{1 + \nu} \frac{J_1^{(r)}}{I_1^{(r)}}\right)^2} + J_{12}^{(r)} \frac{\frac{I_0 + I_1^{(r)}}{I_1^{(r)}}}{\left(2 + \frac{\Delta t_n}{\eta_1} \frac{E_1}{1 + \nu} \frac{J_1^{(r)}}{I_1^{(r)}}\right)^2} \quad (79)$$

where $I_{12}^{(r)}$ and $J_{12}^{(r)}$ are given by (55), and subscript (r) has the same meaning as the one stated in the two previous subsections. Finally let us note that simpler relations than (73), (77), (78) and (79) are obtained if one considers the two non-linear models given by equations (8), (9) and (10). The reader will find them in Royis.¹⁵

5 Numerical computations

This last main section is devoted to the presentation of some numerical results. To begin with, we are interested in a set of computations carried out by using a single four-nodes quadrilateral element for the numerical simulation of homogeneous axisymmetric triaxial compressions tests. These calculations were first performed on APOLLO-DN3000 workstation (DOMAIN OS) from a version of the finite element code ELFIM⁸ running with simple precision, and some of the corresponding results are shown in Royis.^{15,17} In the first of the three following subsections these computations as a whole are reviewed, after renewing them by using the latest version of ELFIM which runs on HP9000 workstation (UNIX OS) with double precision. Then in the second one we deal with the problem of the expanding viscoelastic hollow cylinder, whereas the last subsection is devoted to that of the bending viscoelastic beam.

5.1 Homogeneous triaxial compression path

Here the performances of the three time-discrete schemes described in the previous section are compared by considering numerical simulations of homogeneous axisymmetric triaxial compression tests. In this subsection the sign conventions are those used in soils mechanics (i.e. the compressive stresses are positive and the tensile ones are negative).

For all the computations the total axial strain $\varepsilon_a = 10\%$ is imposed with five equal increments of 2%. Four values of the constant axial strain rate $\dot{\varepsilon}_a$ are considered: 10^{-3}s^{-1} , 10^{-2}s^{-1} , 10^{-1}s^{-1} and 1s^{-1} . The constitutive equations are those of the unified non-linear viscoelastic model given by (9) and (11), and the values of the nine parameters defining this model are the same for all the calculations, except for β_v . The eight constant parameters are given by $E_0 = 867\text{MPa}$, $\nu = 0.3$, $\eta_0 = 500\text{MPa}\cdot\text{s}$, $\alpha_e = 10$, $\beta_2 = \gamma_e = 2$, $\alpha_v = 10^6$ and $\gamma_v = 1$, whereas β_v belongs to the following set of values: $\{0.05, 0.1, 0.2, 0.5, 1, 2, 5\}$. Let us note that all these values are not issued from physical considerations, but that they have been chosen in order to impart high non-linearities to the constitutive model, within the frame of the compression path considered.

The numerical simulations have been carried out, for the four values of the axial strain rate $\dot{\varepsilon}_a$ and for the seven values of the parameter β_v , by using successively scheme S1, scheme S2 with $\theta = 1/2$ (i.e. the classical Crank-Nicolson scheme) and scheme S3. All these 84 calculations have been made by considering a single four-nodes quadrilateral element.

Tables 1-4, relating to each of the four values of $\dot{\varepsilon}_a$, give, for the three previous schemes and for the given values of β_v , the computed values $\sigma_a^{(c)}$ of the axial stress σ_a corresponding to $\varepsilon_a = 10\%$, together with the number of iterations required by each of the five increments.

As shown in the previous section scheme S1 and scheme S2 with $\theta = 1/2$ are not unconditionally superstable so that they can involve oscillations of the numerical solutions. The figure 2 relating to the extreme values of strain rate $\dot{\varepsilon}_a$ and of parameter β_v illustrates this phenomenon.

In order for these two schemes to be less penalized the previous values of $\sigma_a^{(c)}$ in tables 1-4 have been determined, every time such oscillations appeared, by smoothing the last two increments. As to scheme S3, the values are those coming directly from the computations.

Table 1. Number of iterations per increment and values of $\sigma_a^{(c)}$ (MPa): $\dot{\epsilon}_a = 10^{-3} \text{ s}^{-1}$

β_v	Scheme S1		Scheme S2 with $\theta = 1/2$		Scheme S3	
	nb. of it.	$\sigma_a^{(c)}$ (MPa)	nb. of it.	$\sigma_a^{(c)}$ (MPa)	nb. of it.	$\sigma_a^{(c)}$ (MPa)
.05	7-2-3-2-3	.39216 10^{-5}	456-3-436-2-434	.38303 10^{-5}	7-1-1-1-1	.39584 10^{-5}
.1	8-2-3-2-3	.93895 10^{-5}	729-36-808-24-800	.89810 10^{-5}	8-1-1-1-1	.95638 10^{-5}
.2	9-3-5-3-5	.43207 10^{-4}	1108-18-1439-39-1380	.39855 10^{-4}	9-1-1-1-1	.44779 10^{-4}
.5	11-4-8-4-8	.12310 10^{-2}	2434-771-2918-319-2549	.10327 10^{-2}	11-1-1-1-1	.13361 10^{-2}
1.	10-5-10-5-10	.34251 10^{-1}	4738-1090-4221-1458-3894	.24306 10^{-1}	10-3-1-1-1	.39383 10^{-1}
2.	7-5-6-5-6	.78185	4400-159-4292-432-4157	.70772	6-4-3-1-1	.88508
5.	3-3-3-3-2	.13692 10^1	3-2-2-2-2	.13932 10^1	2-2-2-2-1	.15000 10^1

Table 2. Number of iterations per increment and values of $\sigma_a^{(c)}$ (MPa): $\dot{\epsilon}_a = 10^{-2} \text{ s}^{-1}$

β_v	Scheme S1		Scheme S2 with $\theta = 1/2$		Scheme S3	
	nb. of it.	$\sigma_a^{(c)}$ (MPa)	nb. of it.	$\sigma_a^{(c)}$ (MPa)	nb. of it.	$\sigma_a^{(c)}$ (MPa)
.05	7-2-3-2-3	.35142 10^{-4}	451-53-425-2-427	.34325 10^{-4}	7-1-1-1-1	.35473 10^{-4}
.1	8-2-3-2-3	.76160 10^{-4}	760-40-807-2-805	.72855 10^{-4}	8-1-1-1-1	.77575 10^{-4}
.2	9-3-5-3-4	.29436 10^{-3}	1134-22-1440-44-1379	.27154 10^{-3}	9-1-1-1-1	.30508 10^{-3}
.5	11-4-7-4-7	.57152 10^{-2}	2571-634-2918-253-2559	.47970 10^{-2}	11-1-1-1-1	.62034 10^{-2}
1.	11-5-10-4-9	.10971	4293-1121-5007-1405-3876	.79595 10^{-1}	11-3-1-1-1	.12567
2.	8-6-8-6-7	.21907 10^1	6370-1146-5140-784-4609	.21752 10^1	9-4-3-3-1	.24206 10^1
5.	3-3-3-2-2	.14991 10^2	35-12-11-8-5	.14897 10^2	3-3-3-3-3	.14979 10^2

Table 3. Number of iterations per increment and values of $\sigma_a^{(c)}$ (MPa): $\dot{\epsilon}_a = 10^{-1} \text{ s}^{-1}$

β_v	Scheme S1		Scheme S2 with $\theta = 1/2$		Scheme S3	
	nb. of it.	$\sigma_a^{(c)}$ (MPa)	nb. of it.	$\sigma_a^{(c)}$ (MPa)	nb. of it.	$\sigma_a^{(c)}$ (MPa)
.05	7-2-3-2-3	.31493 10^{-3}	447-2-434-2-442	.30760 10^{-3}	7-1-1-1-1	.31789 10^{-3}
.1	8-3-4-3-4	.61765 10^{-3}	818-63-804-2-811	.59105 10^{-3}	8-1-1-1-1	.62924 10^{-3}
.2	9-4-5-3-5	.20052 10^{-2}	1027-17-1452-31-1355	.18506 10^{-2}	9-1-1-1-1	.20785 10^{-2}
.5	10-4-7-3-6	.26530 10^{-1}	2416-603-2905-231-2737	.22540 10^{-1}	10-1-1-1-1	.28797 10^{-1}
1.	10-4-8-5-8	.35215	3572-2293-4388-1985-4127	.32610	11-3-1-1-1	.39857
2.	8-6-7-6-6	.51326 10^1	6481-1191-4146-1695-3634	.52052 10^1	9-4-3-3-3	.54622 10^1
5.	3-3-4-4-4	.68725 10^2	416-2503-2275-1369-770	.69176 10^2	3-3-4-5-4	.68416 10^2

Table 4. Number of iterations per increment and values of $\sigma_a^{(c)}$ (MPa): $\dot{\epsilon}_a = 1 \text{ s}^{-1}$

β_v	Scheme S1		Scheme S2 with $\theta = 1/2$		Scheme S3	
	nb. of it.	$\sigma_a^{(c)}$ (MPa)	nb. of it.	$\sigma_a^{(c)}$ (MPa)	nb. of it.	$\sigma_a^{(c)}$ (MPa)
.05	6-3-3-3-3	.28212 10^{-2}	441-48-427-43-425	.27565 10^{-2}	7-1-1-1-1	.28488 10^{-2}
.1	7-3-4-3-4	.50077 10^{-2}	813-150-793-104-790	.47947 10^{-2}	7-1-1-1-1	.51039 10^{-2}
.2	8-4-5-4-5	.13650 10^{-1}	781-328-1412-186-1406	.12652 10^{-1}	8-1-1-1-1	.14160 10^{-1}
.5	9-4-6-5-6	.12307	2318-851-2771-486-2662	.11083	9-3-1-1-1	.13368
1.	9-5-7-6-6	.11382 10^1	3073-2282-4027-1438-3717	.11147 10^1	9-4-3-1-1	.12615 10^1
2.	6-5-5-5-4	.11648 10^2	5492-2411-3174-2299-2639	.11643 10^2	7-4-3-3-3	.11883 10^2
5.	3-4-3-4-5	.10833 10^3	112-1970-3417-1246-712	.11109 10^3	3-4-3-4-5	.10779 10^3

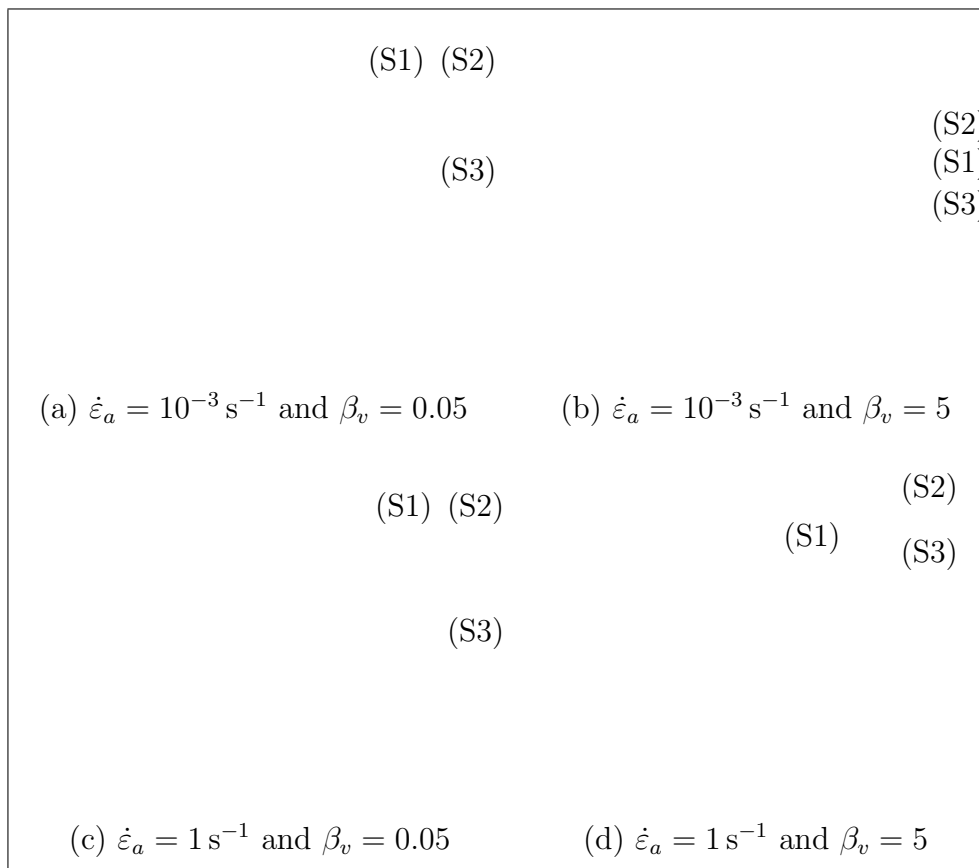


Figure 2. Axial stress $\sigma_a^{(c)}$ versus axial strain ϵ_a

For the compression path considered the tables 1-4 show that scheme S3 requires fewer iterations than scheme S1, whereas scheme S2 with $\theta = 1/2$ is the most demanding. The same is true as regards CPU time. On the other hand reference values $\sigma_a^{(r)}$ of the axial stress σ_a have been determined, for $\epsilon_a = 10\%$ and for each of the values of $\dot{\epsilon}_a$ and β_v considered, by resolving the ordinary differential equation satisfied by σ_a with the first-order fully implicit Euler scheme and successively 10^4 , 10^5 and 10^6 increments, so as to make sure that the first five digits of these numerical solutions given in the table 5 are accurate.

Table 5. Reference values $\sigma_a^{(r)}$ (MPa) of σ_a for $\epsilon = 0.1$

	$\dot{\epsilon} = 10^{-3} \text{ s}^{-1}$	$\dot{\epsilon} = 10^{-2} \text{ s}^{-1}$	$\dot{\epsilon} = 10^{-1} \text{ s}^{-1}$	$\dot{\epsilon} = 1 \text{ s}^{-1}$
$\beta_v = .05$.39584 10^{-5}	.35473 10^{-4}	.31789 10^{-3}	.28488 10^{-2}
$\beta_v = .1$.95638 10^{-5}	.77575 10^{-4}	.62924 10^{-3}	.51039 10^{-2}
$\beta_v = .2$.44779 10^{-4}	.30508 10^{-3}	.20785 10^{-2}	.14161 10^{-1}
$\beta_v = .5$.13361 10^{-2}	.62034 10^{-2}	.28798 10^{-1}	.13368
$\beta_v = 1.$.39382 10^{-1}	.12568	.39857	.12615 10^1
$\beta_v = 2.$.88508	.24206 10^1	.54622 10^1	.11883 10^2
$\beta_v = 5.$.15000 10^1	.14989 10^2	.68430 10^2	.10762 10^3

The tables 6 and 7, in which scheme S2 with $\theta = 1/2$ is simply referenced as S2, give the relative error $\left| \frac{\sigma_a^{(c)} - \sigma_a^{(r)}}{\sigma_a^{(r)}} \right|$ between the computed and reference values of σ_a , for each of the four values of the strain rate $\dot{\epsilon}_a$ and for the seven values of the parameter β_v .

Table 6. Relative errors between $\sigma_a^{(c)}$ and $\sigma_a^{(r)}$: $\dot{\epsilon}_a = 10^{-3} \text{ s}^{-1}$ and $\dot{\epsilon}_a = 10^{-2} \text{ s}^{-1}$

β_v	$\dot{\epsilon}_a = 10^{-3} \text{ s}^{-1}$			$\dot{\epsilon}_a = 10^{-2} \text{ s}^{-1}$		
	Scheme S1	Scheme S2	Scheme S3	Scheme S1	Scheme S2	Scheme S3
.05	.93 10^{-2}	.32 10^{-1}	$< 10^{-5}$.93 10^{-2}	.32 10^{-1}	$< 10^{-5}$
.1	.18 10^{-1}	.61 10^{-1}	$< 10^{-5}$.18 10^{-1}	.61 10^{-1}	$< 10^{-5}$
.2	.35 10^{-1}	.11	$< 10^{-5}$.35 10^{-1}	.11	$< 10^{-5}$
.5	.79 10^{-1}	.23	$< 10^{-5}$.79 10^{-1}	.23	$< 10^{-5}$
1.	.13	.38	.25 10^{-4}	.13	.37	.80 10^{-4}
2.	.11	.20	$< 10^{-5}$.95 10^{-1}	.10	$< 10^{-5}$
5.	.87 10^{-1}	.71 10^{-1}	$< 10^{-5}$.13 10^{-3}	.61 10^{-2}	.67 10^{-3}

Table 7. Relative errors between $\sigma_a^{(c)}$ and $\sigma_a^{(r)}$: $\dot{\epsilon}_a = 10^{-1} \text{ s}^{-1}$ and $\dot{\epsilon}_a = 1 \text{ s}^{-1}$

β_v	$\dot{\epsilon}_a = 10^{-1} \text{ s}^{-1}$			$\dot{\epsilon}_a = 1 \text{ s}^{-1}$		
	Scheme S1	Scheme S2	Scheme S3	Scheme S1	Scheme S2	Scheme S3
.05	.93 10^{-2}	.32 10^{-1}	$< 10^{-5}$.97 10^{-2}	.32 10^{-1}	$< 10^{-5}$
.1	.18 10^{-1}	.61 10^{-1}	$< 10^{-5}$.19 10^{-1}	.61 10^{-1}	$< 10^{-5}$
.2	.35 10^{-1}	.11	$< 10^{-5}$.36 10^{-1}	.11	.71 10^{-4}
.5	.79 10^{-1}	.22	.35 10^{-4}	.79 10^{-1}	.17	$< 10^{-5}$
1.	.12	.18	$< 10^{-5}$.98 10^{-1}	.12	$< 10^{-5}$
2.	.60 10^{-1}	.47 10^{-1}	$< 10^{-5}$.20 10^{-1}	.20 10^{-1}	$< 10^{-5}$
5.	.43 10^{-2}	.11 10^{-1}	.20 10^{-3}	.66 10^{-2}	.32 10^{-1}	.16 10^{-2}

They illustrate (for the compression path considered) the accuracy of scheme S3, especially for the lowest values of parameter β_v thus increasing the non-linear feature of the constitutive model, as shown in the table 8 giving, for the reference stresses $\sigma_a^{(r)}$, the values of the non-linear term $\alpha_v \left(\frac{\|\mathbf{S}\|}{E_0} \right)^{\beta_v}$ appearing in expression (11) of η .

Finally table 9 gives, for the same reference stresses, the values of ratio ρ similar to that introduced in the previous section and defined by $\rho = \Delta t / \tau$, where $\Delta t = 0.02 / \dot{\epsilon}_a$ is the time step and τ the relaxation time obtained by $\tau = \frac{3}{2} \eta / E$ from the expressions (11) of E and η . These values of ρ together with the considerations made in the previous section account for the oscillating behaviour of the numerical solutions coming from schemes S1 and S2.

Table 8. Values of the non-linear term $\alpha_v \left(\frac{\|\mathbf{s}\|}{E_0} \right)^{\beta_v}$ for the reference stresses $\sigma_a^{(r)}$

	$\dot{\epsilon} = 10^{-3} s^{-1}$	$\dot{\epsilon} = 10^{-2} s^{-1}$	$\dot{\epsilon} = 10^{-1} s^{-1}$	$\dot{\epsilon} = 1 s^{-1}$
$\beta_v = .05$.37894 10^6	.42286 10^6	.47186 10^6	.52654 10^6
$\beta_v = .1$.15684 10^6	.19336 10^6	.23838 10^6	.29389 10^6
$\beta_v = .2$.33497 10^5	.49167 10^5	.72167 10^5	.10593 10^6
$\beta_v = .5$.11217 10^4	.24170 10^4	.52077 10^4	.11220 10^5
$\beta_v = 1.$.37088 10^2	.11835 10^3	.37535 10^3	.11880 10^4
$\beta_v = 2.$.69476	.51967 10^1	.26461 10^2	.12523 10^3
$\beta_v = 5.$.56251 10^{-8}	.56048 10^{-3}	.11115 10^1	.10695 10^2

Table 9. Values of the ratio $\rho = \Delta t/\tau$ for the reference stresses $\sigma_a^{(r)}$

	$\dot{\epsilon} = 10^{-3} s^{-1}$	$\dot{\epsilon} = 10^{-2} s^{-1}$	$\dot{\epsilon} = 10^{-1} s^{-1}$	$\dot{\epsilon} = 1 s^{-1}$
$\beta_v = .05$.65709 10^7	.73323 10^6	.81820 10^5	.91302 10^4
$\beta_v = .1$.27196 10^7	.33529 10^6	.41336 10^5	.50961 10^4
$\beta_v = .2$.58085 10^6	.85257 10^5	.12514 10^5	.18368 10^4
$\beta_v = .5$.19468 10^5	.41929 10^4	.90319 10^3	.19457 10^3
$\beta_v = 1.$.66045 10^3	.20696 10^3	.65259 10^2	.20619 10^2
$\beta_v = 2.$.29388 10^2	.10746 10^2	.47643 10^1	.21943 10^1
$\beta_v = 5.$.17341 10^2	.17419 10^1	.39718	.24659

5.2 Expanding viscoelastic hollow cylinder

In this subsection we are interested in the expanding viscoelastic hollow cylinder shown on the figure 3. The problem is studied over the time interval $[0, T]$, and the boundary conditions relating to time $t \in [0, T]$ are given in this figure.

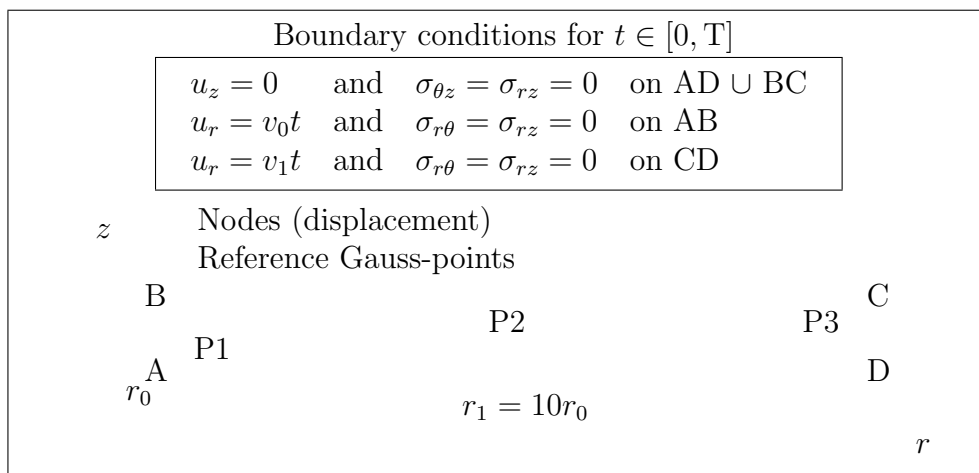


Figure 3. Expanding viscoelastic hollow cylinder

The behaviour of the viscoelastic cylinder is described by an isotropic Maxwell model, the constitutive equations of which are as follows

$$\dot{\varepsilon}(t) = \frac{-\nu}{E} \text{tr} \dot{\sigma}(t) \mathbf{I}_2 + \frac{1+\nu}{E} \dot{\sigma}(t) + \frac{-\nu}{\eta} \text{tr} \sigma(t) \mathbf{I}_2 + \frac{1+\nu}{\eta} \sigma(t) \quad (80)$$

Using cylindrical coordinates (r, θ, z) the only non-zero component u_r of the displacement field \mathbf{u} does not depend on z and is given by

$$u_r(t, r) = \left(\frac{v_1 r_1 - v_0 r_0}{r_1^2 - r_0^2} r + \frac{v_0 r_1 - v_1 r_0}{r_1^2 - r_0^2} \frac{r_0 r_1}{r} \right) t \quad (81)$$

For $v_1 = v_0 r_0 / r_1 = v_0 / 10$ this exact solution is identical to that of the problem of the expanding infinite viscoelastic hollow cylinder ($r_1 = +\infty$). By restricting the study to this particular expression of v_1 we get the following expressions of the non-zero components of \mathbf{u} , ε and σ

$$\begin{cases} u_r(t, r) &= \frac{r_0}{r} v_0 t \\ \varepsilon_{rr}(t, r) &= -\varepsilon_{\theta\theta}(t, r) = -\frac{r_0}{r^2} v_0 t \\ \sigma_{rr}(t, r) &= -\sigma_{\theta\theta}(t, r) = -\frac{\eta}{1+\nu} \frac{r_0}{r^2} v_0 \left(1 - \exp\left(\frac{-t}{\tau}\right) \right) \end{cases} \quad (82)$$

where $\tau = \eta/E$ stands for relaxation time.

21 numerical computations have been carried out by considering as in the previous subsection scheme S1, scheme S2 with $\theta = 1/2$ and scheme S3 together with seven different values of the constant time step: $\Delta t = T/N$ with $N \in \{1, 2, 5, 10, 20, 50, 100\}$. All these simulations have been performed by using the same mesh composed of nine 12-nodes (cubic) quadrilateral elements of the ‘serendipity’ family (see figure 3), and for the various parameters the following values: $T = 10$ s, $r_0 = 1$ m, $v_0 = 10^{-2}$ ms⁻¹, $E = 1000$ MPa, $\nu = 0.3$ and $\eta = 1000$ MPa.s.

As shown in the previous section the use of scheme S1 and scheme S2 with $\theta = 1/2$ for the time discretization of the constitutive equations (80) leads to the same approximation and the computations reflect this feature, so that only schemes S1 and S3 are considered in the following. Three reference Gauss-points denoted as P1, P2 and P3 and shown on figure 3 have been chosen for the analysis of the numerical results relating to $t = T = 10$ s. For these three points, for the two schemes S1 and S3 and for the seven values of the time step Δt the table 10 gives the relative error $\left| \frac{\sigma_{rr}^{(c)} - \sigma_{rr}^{(e)}}{\sigma_{rr}^{(e)}} \right|$ between the computed values $\sigma_{rr}^{(c)}$ of the radial stress σ_{rr} and the exact ones $\sigma_{rr}^{(e)}$, whereas the same analysis is made in table 11 for the orthoradial stress $\sigma_{\theta\theta}$.

Table 10. Relative errors between $\sigma_{rr}^{(c)}$ and $\sigma_{rr}^{(e)}$ for $t = 10$ s

Δt (s)	Gauss-point P1		Gauss-point P2		Gauss-point P3	
	Scheme S1	Scheme S3	Scheme S1	Scheme S3	Scheme S1	Scheme S3
.1	.85 10^{-1}	.85 10^{-1}	.40 10^{-1}	.40 10^{-1}	.12 10^{-1}	.12 10^{-1}
.2	.85 10^{-1}	.85 10^{-1}	.40 10^{-1}	.40 10^{-1}	.12 10^{-1}	.12 10^{-1}
.5	.85 10^{-1}	.85 10^{-1}	.40 10^{-1}	.40 10^{-1}	.12 10^{-1}	.12 10^{-1}
1.	.85 10^{-1}	.85 10^{-1}	.40 10^{-1}	.40 10^{-1}	.12 10^{-1}	.12 10^{-1}
2.	.85 10^{-1}	.85 10^{-1}	.40 10^{-1}	.40 10^{-1}	.11 10^{-1}	.12 10^{-1}
5.	.11	.82 10^{-1}	.22	.43 10^{-1}	.19	.14 10^{-1}
10.	.81	.67 10^{-1}	.60	.56 10^{-1}	.65	.28 10^{-1}

Table 11. Relative errors between $\sigma_{\theta\theta}^{(c)}$ and $\sigma_{\theta\theta}^{(e)}$ for $t = 10$ s

Δt (s)	Gauss-point P1		Gauss-point P2		Gauss-point P3	
	Scheme S1	Scheme S3	Scheme S1	Scheme S3	Scheme S1	Scheme S3
.1	.13	.13	.39 10^{-1}	.39 10^{-1}	.12 10^{-1}	.12 10^{-1}
.2	.13	.13	.39 10^{-1}	.39 10^{-1}	.12 10^{-1}	.12 10^{-1}
.5	.13	.13	.39 10^{-1}	.39 10^{-1}	.12 10^{-1}	.12 10^{-1}
1.	.13	.13	.39 10^{-1}	.39 10^{-1}	.12 10^{-1}	.12 10^{-1}
2.	.13	.13	.39 10^{-1}	.39 10^{-1}	.12 10^{-1}	.12 10^{-1}
5.	.77 10^{-1}	.13	.22	.42 10^{-1}	.19	.15 10^{-1}
10.	.89	.11	.60	.55 10^{-1}	.65	.28 10^{-1}

These relative errors illustrate the considerations of the previous section relating to the superstability properties of the schemes considered. And indeed the relative errors coming from the scheme S1 increase strongly when the ratio $\rho = \Delta t/\tau$ becomes greater than 2 (here the values of ρ and Δt are identical since $\tau = \eta/E = 1$ s), whereas those coming from scheme S3 are slightly modified by the raising of the time step size.

On the other hand, note that for the two schemes and for all the values of ρ less than or equal to 2, then the relative errors are the same and decrease when r increases. This lies in the fact that these errors for their most part come from space approximation and not from time discretization. And indeed the shape functions used for the approximation of the radial displacement u_r are polynomials of degree 3 in r , whereas the exact expression (82) of u_r is inversely proportional to r .

5.3 Bending viscoelastic beam

In this last subsection we consider the bending viscoelastic beam shown on figure 4. The problem is studied for $t \in [0, T]$ and the essential boundary conditions are given by

$\mathbf{u} = 0$ on $AB \times [0, T]$, whereas the vertical load P applied to point C (see figure 4) remains constant for $t \in [0, T]$.

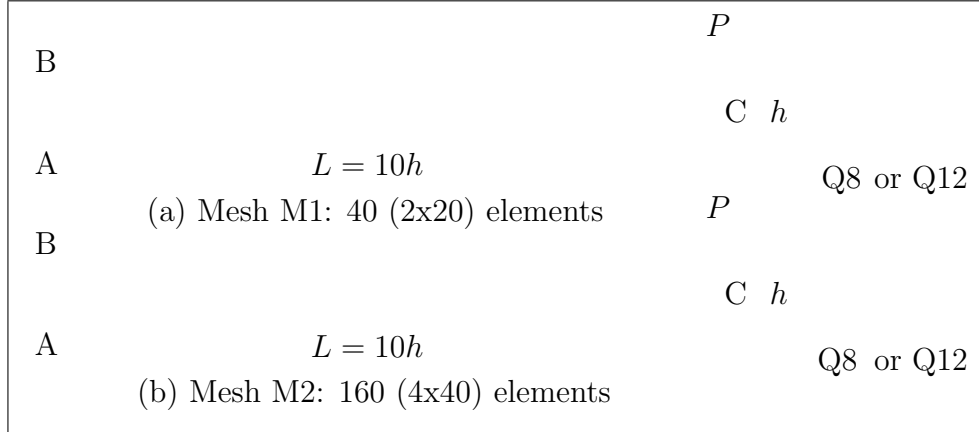


Figure 4. Bending Viscoelastic Beam

The viscoelastic behaviour of the beam is now described by an isotropic Kelvin-Voigt model, the constitutive equations of which are

$$\sigma(t) = \frac{E\nu}{(1+\nu)(1-2\nu)} \text{tr}\varepsilon(t)\mathbf{I}_2 + \frac{E}{1+\nu}\varepsilon(t) + \frac{\eta\nu}{(1+\nu)(1-2\nu)} \text{tr}\dot{\varepsilon}(t)\mathbf{I}_2 + \frac{\eta}{1+\nu}\dot{\varepsilon}(t) \quad (83)$$

According to the theory of continuous beams we shall restrict the study to the case $\nu = 0$, so that the previous equation (83) becomes

$$\sigma(t) = E\varepsilon(t) + \eta\dot{\varepsilon}(t) \quad (84)$$

Let us denote as $V(t)$, $t \in [0, T]$, the vertical displacement of point C in the direction of load P . Then the theory of continuous beams leads to the following expression of $V(t)$

$$V(t) = \frac{4PL^3}{Ebh^3} \left(1 - \exp\left(\frac{-t}{\tau}\right)\right) \quad (85)$$

where b is the width of the beam and $\tau = \eta/E$ the relaxation time.

The numerical computations have been carried out by considering the two meshes M1 and M2 shown on figure 4 and made up of 40 and 160 square elements, respectively. For both of these meshes the 8-nodes (quadratic) and 12-nodes (cubic) quadrilateral elements of the ‘serendipity’ family (see again figure 4) have been used successively. In all the following the four resulting finite element meshes of the beam are denoted as M1Q8, M1Q12, M2Q8 and M2Q12. They have a total of 320, 520, 1120 and 1840 degrees of freedom, respectively. 48 numerical simulations have been performed by considering these four meshes, schemes S1, S2 with $\theta = 1/2$ and S3,

together with four different values of the constant time step: $\Delta t = T/N$ with $N \in \{1, 2, 5, 10\}$. All these computations have been carried out by using the following values of the various parameters: $T = 10$ s, $b = h = 1$ m, $P = 10^3$ kN, $E = 12000$ MPa and $\eta = 12000$ MPa.s.

For the four meshes, for the three schemes S1, S2 and S3 (in all the following the scheme S2 with $\theta = 1/2$ is simply referenced as S2) and for the four values of the time step Δt , the tables 12 and 13 give the relative errors $\left| \frac{V^{(c)} - V^{(a)}}{V^{(a)}} \right|$ between the computed values $V^{(c)}$ of the vertical displacement $V(t)$ of point C at time $t=T=10$ s and the analytical ones $V^{(a)}$ at the same time given by relation (85).

Table 12. Relative errors between $V^{(c)}$ and $V^{(a)}$: Meshes M1Q8 and M1Q12

Δt (s)	Mesh M1Q8			Mesh M1Q12		
	Scheme S1	Scheme S2	Scheme S3	Scheme S1	Scheme S2	Scheme S3
1.	.61 10^{-2}	.61 10^{-2}	.60 10^{-2}	.61 10^{-2}	.62 10^{-2}	.61 10^{-2}
2.	.61 10^{-2}	.62 10^{-2}	.58 10^{-2}	.61 10^{-2}	.62 10^{-2}	.59 10^{-2}
5.	.61 10^{-2}	.18	.32 10^{-2}	.61 10^{-2}	.18	.32 10^{-2}
10.	.61 10^{-2}	.68	.10 10^{-1}	.61 10^{-2}	.68	.10 10^{-1}

Table 13. Relative errors between $V^{(c)}$ and $V^{(a)}$: Meshes M2Q8 and M2Q12

Δt (s)	Mesh M2Q8			Mesh M2Q12		
	Scheme S1	Scheme S2	Scheme S3	Scheme S1	Scheme S2	Scheme S3
1.	.62 10^{-2}	.61 10^{-2}	.61 10^{-2}	.63 10^{-2}	.63 10^{-2}	.62 10^{-2}
2.	.62 10^{-2}	.62 10^{-2}	.59 10^{-2}	.63 10^{-2}	.63 10^{-2}	.60 10^{-2}
5.	.62 10^{-2}	.18	.33 10^{-2}	.62 10^{-2}	.18	.34 10^{-2}
10.	.62 10^{-2}	.68	.10 10^{-1}	.62 10^{-2}	.68	.10 10^{-1}

As in the previous subsection for the viscoelastic hollow cylinder the relative errors relating to scheme S2 increase strongly when the ratio $\rho = \Delta t/\tau$ becomes greater than 2 (the values of ρ and Δt are again identical since $\tau = \eta/E = 1$ s), whereas the same does not hold for S1 anymore since the errors coming from this scheme are now independent of the values of $\rho \in \{1, 2, 5, 10\}$. On the other hand the relative errors relating to scheme S3 are now a little bit more influenced by the raising of the time step size than those obtained in the previous subsection for the viscoelastic hollow cylinder.

This good behaviour of scheme S1 lies in the fact that the components of the Cauchy stress tensor σ remain time-independent, so that assumption 1 is here exactly satisfied. Let us note finally that the relative errors above are not much modified by the size of the mesh.

6 Concluding remarks

Robust time-discrete schemes are needed for the finite element modelling of mechanical problems involving viscous materials, if one wants to obtain accurate numerical approximations at a reasonable cost. As to the linear and non-linear viscoelastic constitutive equations considered in this paper, the second-order scheme denoted as S3 and described in the previous sections meets this robustness requirement, in the sense that the resulting numerical approximations remain superstable even when large values of the time step are taken. This unconditional superstability of S3, which is easy to prove if one restricts the study to linear ordinary differential equations, is illustrated by the numerical results presented in the last section. Nevertheless it is obvious that other computations are needed in order to confirm the apparent robustness of S3 when used for the numerical integration of the viscoelastic constitutive equations considered. On the other hand we have to bear in mind that the bringing into play of scheme S3 is strongly linked to the particular forms of these equations, so that the previous remarks relating to the robustness of S3 hold only for them and are not directly transposable to other viscous models.

REFERENCES

1. J. Mandel, *Cours de Mécanique des Milieux Continus Tome 2*, Gauthier & Villars Ed., Paris, 1966.
2. S.W. Sloan, 'Substepping schemes for the numerical integration of elastoplastic stress-strain relations', *Int. j. numer. methods eng.*, **24**, 893-911 (1987).
3. S.W. Sloan and J.R. Booker, 'Integration of Tresca and Mohr-Coulomb constitutive relations in plane strain elastoplasticity', *Int. j. numer. methods eng.*, **33**, 163-196 (1992).
4. T.J.R. Hughes and R.L. Taylor, 'Unconditionally stable algorithms for quasi-static elasto/visco-plastic finite element analysis', *Comp. Struct.*, **8**, 169-173 (1978).
5. M.L. Wenner, 'A generalized forward gradient procedure for rate sensitive constitutive equations', *Int. j. numer. methods eng.*, **36**, 985-995 (1993).
6. H.H. Rosenbrock, 'Some general implicit processes for the numerical solution of differential equations', *Comp. J.*, **5**, 329-330 (1963).
7. A. Curnier, *Méthodes Numériques en Mécanique des Solides*, Presses Polytechniques et Universitaires Romandes, Lausanne, 1993.
8. P. Royis, Formulation mathématique de lois de comportement - Modélisation numérique de problèmes aux limites en mécanique des solides déformables, Thèse de Doctorat d'Ingénieur, spécialité Mécanique, Institut National Polytechnique de Grenoble, 1986.

9. A. Friaâ, La loi de Norton-Hoff généralisée en plasticité et viscoplasticité, Thèse de Doctorat ès Sciences Mathématiques, Université Pierre et Marie Curie Paris VI, 1979.
10. H. Di Benedetto, Modélisation du comportement des géomatériaux - Application aux enrobés et aux bitumes, Thèse de Doctorat ès Sciences Physiques, Université Scientifique et Médicale de Grenoble, 1987.
11. P. Royis, P., An original time-discrete scheme for viscoelastic and viscoplastic problems, In *Proceedings of the 2nd European Specialty Conference on Numerical Methods in Geotechnical Engineering*, Ed. by CEDEX, Santander, pp. 145-154, 1990.
12. W. Kutta, 'Betreig zur näherungsweise integration totaler differentialgleichungen', *Z. Math. Phys.*, **46**, 435-453 (1901).
13. H. Crouzeix and A.L. Mignot, *Analyse Numérique des Equations Différentielles*, Masson Ed., Paris, 1989.
14. P.C. Hammer and J.W. Hollingsworth, 'Trapezoidal methods of approximating solutions of differential equations', *Math. Comp.*, **9**, 92-96 (1955).
15. P. Royis, Modélisation par éléments finis des géomatériaux, Thèse d'Habilitation à diriger des Recherches, Institut National Polytechnique de Grenoble, 1995.
16. P. Royis, Influence des schémas discrets en temps sur les solutions numériques en viscoélasticité et viscoplasticité, In: *Rapport scientifique du GRECO Géomatériaux - Groupe modèles numériques*, Ed. by J.M. Reynouard, Grenoble, pp. 484-488, 1988.
17. P. Royis, Integration by FEM of viscous models: a comparison between three time-discrete schemes, In: *Proceedings of the 5th International Symposium on Numerical Models in Geomechanics*, Ed. by G.N. Pande and S. Pietruszczak, A.A. Balkema, Rotterdam, pp. 423-428, 1990.